International Journal of Biological Macromolecules 253 (2023) 126933

Contents lists available at ScienceDirect

International Journal of Biological Macromolecules

journal homepage: www.elsevier.com/locate/ijbiomac

Fabrication and characterization of new levan@CBD biocomposite sponges as potential materials in natural, non-toxic wound dressing applications

Dorota Chelminiak-Dudkiewicz [a,*], Miloslav Machacek [b], Jolanta Dlugaszewska [c], Magdalena Wujak [d], Aleksander Smolarkiewicz-Wyczachowski [a], Szymon Bocian [e], Kinga Mylkie [a], T. Goslinski [f], Michal P. Marszall [d], Marta Ziegler-Borowska [a,*]

[a] Department of Biomedical Chemistry and Polymer Science, Faculty of Chemistry, Nicolaus Copernicus University in Torun, Gagarina 7, 87-100 Torun, Poland
[b] Department of Biochemical Sciences, Faculty of Pharmacy in Hradec Kralove, Charles University in Prague, Akademika Heyrovskeho 1203, 500-05 Hradec Kralove, Czech Republic
[c] Department of Genetics and Pharmaceutical Microbiology, Poznan University of Medical Sciences, Rokietnicka 3, 60-806 Poznan, Poland
[d] Department of Medicinal Chemistry, Faculty of Pharmacy, Collegium Medicum in Bydgoszcz, Nicolaus Copernicus University in Torun, Jurasza 2, 85-089 Bydgoszcz, Poland
[e] Department of Environmental Chemistry and Bioanalysis, Faculty of Chemistry, Nicolaus Copernicus University in Torun, Gagarina 7, 87-100 Torun, Poland
[f] Chair and Department of Chemical Technology of Drugs, Poznan University of Medical Sciences, Grunwaldzka 10, 60-780 Poznan, Poland

ARTICLE INFO

Keywords:
Levan
cannabis oil
Antibacterial activity
In vitro biocompatibility test
Wound dressing

ABSTRACT

Wound healing is a complex process; therefore, new dressings are frequently required to facilitate it. In this study, porous bacterial levan-based sponges containing cannabis oil (Lev@CBDs) were prepared and fully characterized. The sponges exhibited a suitable swelling ratio, proper water vapor transmission rate, sufficient thermal stability, desired mechanical properties, and good antioxidant and anti-inflammatory properties. The obtained Lev@CBD materials were evaluated in terms of their interaction with proteins, human serum albumin and fibrinogen, of which fibrinogen revealed the highest binding effect. Moreover, the obtained biomaterials exhibited antibacterial activity against *Staphylococcus aureus* and *Pseudomonas aeruginosa*, as well as being non-hemolytic material as indicated by hemolysis tests. Furthermore, the sponges were non-toxic and compatible with L929 mouse fibroblasts and HDF cells. Most significantly, the levan sponge with the highest content of cannabis oil, in comparison to others, retained its non-hemolytic, anti-inflammatory, and antimicrobial properties after prolonged storage in a climate chamber at a constant temperature and relative humidity. The designed sponges have conclusively proven their beneficial physicochemical properties and, at the preliminary stage, biocompatibility as well, and therefore can be considered a promising material for wound dressings in future *in vivo* applications.

1. Introduction

A wound is defined as an injury or disruption of the anatomical structure and function of the tissues, such as the skin. Wounds that heal completely within twelve weeks with the least amount of scarring are called acute, while those that are recurring and take a long time to cure may be classified as chronic [1,2]. Wound healing is a complex process, and microbial infection can complicate it. Wounds with compromised skin integrity should usually be covered with a wound dressing material to minimize loss of function [3]. Several studies have shown that an ideal wound dressing should present the following attributes: biocompatibility, adequate water vapor transmission rate (WVTR) - porous structure, inhibit microbial growth, non-toxic, and non-allergenic. The easy and painless removal of the wound dressing is also of great importance [4–8]. Wound dressing materials can be prepared in various forms, such as films [9–11], hydrogels [12–15], nanofibers [16–18], and sponges [19–22]. Sponge dressings are notably soft, flexible and have a high swelling capacity and porosity. It has been shown that a sponge with pores tens to hundreds of microns in diameter can enhance tissue growth [23]. In addition, sponges that contain a sufficient amount of water provide a moist environment, thus a barrier to bacterial infections. It is worth noting that sponges with 3D porous

* Corresponding authors.
E-mail addresses: dorotachd@umk.pl (D. Chelminiak-Dudkiewicz), martaz@umk.pl (M. Ziegler-Borowska).

https://doi.org/10.1016/j.ijbiomac.2023.126933
Received 7 August 2023; Received in revised form 9 September 2023; Accepted 14 September 2023
Available online 16 September 2023

structures can also be loaded with various bioactive substances (for example, antibacterial, anti-inflammatory, antioxidants, *etc.*).

Dressing materials can be composed of natural and synthetic polymers and their combinations. However, natural polymers are more suitable candidates for wound dressing materials due to their unique properties, such as feasible topography, high porosity, and biocompatibility. Moreover, these polymers are characterized by their morphological similarity to the extracellular matrix, thus minimizing the risk of immunological reactions often detected with synthetic polymers [24–26].

Polysaccharides constitute a significant group of naturally occurring polymers. They are also known as glycans and consist of monosaccharide subunits (and/or their derivatives). The main advantage of polysaccharides is their chemical similarity to glycosaminoglycans such as heparin, keratan sulfate, and hyaluronan, which gives them good biocompatibility, including hemocompatibility [27]. They are composed of one type of monosaccharide subunits known as homopolysaccharides, while those consisting of two or more types of monosaccharides are named heteropolysaccharides [28]. One example of homopolysaccharides is bacterial levan (Lev), which consists of polyfructose chains capped by glucose residues. It is a non-toxic, biocompatible, and strongly adhesive polysaccharide [29–31]. As an uncharged polysaccharide with good physical properties, levan can potentially be used as a blood plasma substitute, extender, anticancer and antihyperlipidemic agent [32,33]. Moreover, it reveals anti-irritant, antioxidant, and anti-inflammatory properties, making this biopolymer a good candidate for wound treatment. However, there needs to be more information in the literature on using a levan sponge as a potential dressing material. Furthermore, using this polysaccharide combined with the well-studied chitosan can improve dressing properties, positively influencing wound healing.

In addition, plant extract composites containing natural active ingredients are becoming increasingly popular due to the spread of antimicrobial resistance and side effects of synthetic antibiotics. One of them is Cannabis oil (CBD), a popular remedy in alleviating many ailments and treating diseases for some time. It is recommended for treating pain (including chronic and cancer-related), autoimmune diseases, mental illnesses, and others due to its naturalness [34–36]. Cannabis oil has no addictive or intoxicating effects, so many people can successfully supplement it [37]. CBD has a complex legal status that varies from country to country and region to region. In Poland, products derived from industrial hemp with a THC content of <0.2 % (according to European Union regulations) can be legal and available on the market. Cannabis oils from such hemp are usually considered food products or dietary supplements, and their sale and possession are permitted. The primary active substance of the oil is non-psychoactive cannabidiol, which has beneficial analgesic, antioxidant, antibacterial, anti-inflammatory, and regenerative properties. Therefore, it can be an excellent additive to dressing materials, improving wound healing and reducing scarring. Importantly, mammals possess an endocannabinoid system whose central role is maintaining homeostasis throughout the body. This system includes, among others, two receptors: CB1 (present in the brain, adipose tissue, skeletal muscles, liver, and lungs) and CB2 (located mainly on the immune system cells), which combine with cannabinoids acting on them. Each receptor is adapted to work with both physiologically produced endocannabinoids, *e.g.*, anandamide, 2-arachidonoyl glycerol [38], and those from exogenous sources (phytocannabinoids). If endocannabinoid transmission fails, phytocannabinoids can then replace them. Cannabidiol stimulates the endocannabinoid system's activity and thus restores balance, so its use in wound dressings is fully justified [39,40]. Moreover, CBD oil is thought to have a perfect balance (3:1) ratio of the essential polyunsaturated fatty acids (linoleic acid and linolenic acid). Due to this property, the oil penetrates easily into the skin [41,42]. In our previous work, we obtained films based on chitosan with CBD oil [11]. These materials met most of the characteristics required to be a good wound dressing material (such as rough surface, non-toxicity, antimicrobial, *etc.*).

To the best of our knowledge, there are very few reports in the literature on polysaccharide composites with cannabidiol for wound treatment. Zheng and co-authors [43] obtained an alginate-based hydrogel containing cannabidiol, characterized by good biocompatibility, antibacterial activity, and angiogenesis properties. Monou and co-authors [44] described the synthesis and characteristic 3D-printed alginate films with cannabidiol (CBD) and cannabigerol (CBG) nanoparticles for potential wound healing applications. Antezan's team [45] described a novel 3D-printed gelatin-alginate scaffold with hemp seed oil, suggesting that this material could become an attractive alternative to common soft tissue infection and wound repair treatments. The same team also described collagen hydrogels enriched with *cannabis sativa* [46]. Nonetheless, combining polysaccharide composites with CBD for wound treatment is relatively new and requires much investigation.

The study presents the preparation of novel levan sponges enriched with cannabis oil (Lev@CBD) to promote wound healing. Systematical characterizations of the obtained biomaterial were performed, including the surface morphology, chemical structure, thermal stability, mechanical performance, and the release of CBD. Moreover, the samples were placed in an aging chamber for 3 months to evaluate their stability under certain atmospheric conditions. The biological effect of the sponge was also assessed, and according to the results, the material exhibited excellent anti-inflammatory, antioxidant, and antimicrobial properties. Interestingly, all the data suggest that Lev@CBD sponges can act as a novel multifunctional dressing for wound healing without significantly decreasing activity during storage under harsh conditions.

2. Materials and methods

2.1. Materials

Levan from *Erwinia herbicola* (molecular weight $1.3*10^6$ Da), sodium periodate, phosphate buffer saline (PBS) (pH 7.4), diclofenac sodium, human serum albumin (HSA), bovine serum albumin (BSA), fibrinogen, lysozyme, and 2,2-diphenyl-1-picrylhydrazyl radical (DPPH) were purchased from Sigma-Aldrich (Munich, Germany). Acetic acid, acetone, dimethylformamide, sodium hydroxide, hydrochloric acid, and phenolphthalein were purchased from Avantor Performance Materials Poland s.a. (formerly POCH; Gliwice, Poland). Cannabis oil (20 % of CBD in oil; CBD Pure) was purchased from a local pharmacy. Reagents for the antibacterial tests: Microbank cryogenic vials (ProLabDiagnostics, Canada), Brain Heart Infusion Broth (Oxoid, UK), Tryptone Soya Agar (Oxoid, UK), Sodium chloride (Avantor Performance Materials Poland S.A., Poland).

All reagents for the fibroblast cell culture: Eagle's Minimum Essential Medium (EMEM), fetal bovine serum (FBS), Non-Essential Amino Acids (NEAA), L-glutamine, trypsin-EDTA, penicillin/streptomycin solution, Dulbecco's phosphate buffer saline (DPBS) were purchased from Biowest (Nuaillé, France). 2-isopropanol, hydrochloric acid, and MTT (3-(4,5-dimethylthiazol-2-yl)-2,5-diphenyltetrazolium bromide; suitable for cell culture) were purchased from Sigma-Aldrich. All reagents were used without additional purification.

2.2. Preparation of levan sponges enriched with cannabis oil (Lev@CBD)

Levan from *Erwinia herbicola* (0.1 g) was mechanically stirred (600 rpm) in acetic acid solution (C = 1 %, 10 mL) at room temperature. Then, CBD oil (1.0 % by weight to levan) was added, and the stirring continued for 30 min. Subsequently, the mixture was centrifuged (to remove the bubbles), cast into a 24-well plate (15.5 mm diameter) or 96-well plate (6.58 mm diameter), frozen (−20 °C, 6 h), and lyophilized overnight in a freeze dryer (−51 °C, 0.031 mBar).

Levan sponges with cannabis oil at higher concentrations (10.0 % and 20.0 % by weight to levan) were obtained using the same method. The groups of sponges rendered were designated as Lev@1CBD,

Lev@10CBD, and Lev@20CBD, for 1 %, 10 %, and 20 % of cannabis oil content, respectively.

2.3. Characterization of levan sponges enriched with cannabis oil (Lev@CBDs)

2.3.1. Attenuated total reflectance spectroscopy (ATR-FTIR)

Structures of the pure levan, cannabis oil, and Lev@CBD sponges were characterized by the Attenuated Total Reflectance Fourier Transform Infrared (ATR-FTIR) spectroscopy with Spectrum Two™ (Perkin Elmer, Waltham, MA, USA) apparatus equipped with the diamond crystal. Spectra were recorded in the range of 4000 to 450 cm^{-1} at a resolution of 4 cm^{-1}, and 64 scans. After recording the spectra, the baseline and ATR corrections were made.

2.3.2. Scanning electron microscopy

The morphology of the obtained Lev@CBD sponges was studied with a Scanning Electron Microscope (1430 VP LEO Electron Microscopy Ltd.).

2.3.3. Thermogravimetric analysis (TGA)

Thermal gravimetric analysis of the levan, cannabis oil, and Lev@CBD sponges was performed on a TA Instruments (SDT 2960 Simultaneous DSC-TGA thermogravimetric analyzer) at a 10 °C/min heating rate in the range from ambient to 600 °C in the atmosphere of nitrogen. We chose the temperature range based on our previous works [11,47]. Above 600 °C, no changes were observed.

2.3.4. Mechanical and adhesive properties

The mechanical properties of levan and Lev@CBD sponges were tested by the EZ-Test E2-LX Shimadzu texture analyzer (Shimadzu, Kioto, Japan) at room temperature (RT). Three sample strips of the sponges were cut and clamped between pneumatic grips. The tests were performed at an extension rate of 20 mm/min, and each sample was repeated three times.

The universal testing machine was also applied to measure the adhesive strength of the sponges. According to the literature [48–50] the substrate (glass slide) bonded with the levan and Lev@CBD sponges (10 mm x10 mm) and compressed for several minutes at room temperature. The test were performed at an extension rate of 20 mm/min, and each sample was repeated three times.

2.3.5. Swelling analysis

The swelling ratio of the prepared biomaterials was calculated by incubating Lev@CBD sponges (each sponge weighed about 0.2 g) in PBS solution (4 mL) pH 5.6 and pH 7.4 at 37 °C to mimic bodily conditions. After wiping excess water, the sponges were weighed regularly. This experiment was performed in triplicate. The swelling rate was calculated using Formula 1 shown bellow:

$$Swelling\ rate\ (\%) = \frac{(W_s - W_D)}{W_D} * 100\% \quad (1)$$

where, Ws is the weight of the swollen sample and WD is the weight of dried sample [51].

2.3.6. Biodegradation test

Biodegradation profiles of the Lev@CBD sponges were determined by monitoring their weight changes for 14 days, according to previous reports [52]. A known weight of the sponges was incubated in PBS (pH = 7.4, 37 °C) containing lysozyme (0.5 mg/mL). Immersed sponges were taken out daily, washed with deionized water, and freeze-dried. The biodegradability of the sponges was calculated using Formula 2, shown below:

$$Biodegradation\ (\%) = \frac{(W_0 - W)}{W_0} * 100\% \quad (2)$$

where, W_0 is the initial weight of the sponge and W is the final weight of the sponge [52,53].

2.3.7. Porosity

First, sponges were dried at 50 °C for 2 h in a vacuum oven. Next, the weighed sponges (0.2 g) were immersed for 4 h in absolute ethanol (4 mL). After that, the swollen sponges were then blotted to eliminate the extra ethanol using filter paper and weighed. The porosity of the sponges was calculated using Formula 3 shown below:

$$\text{Porosity}\ (\%) = \frac{(\mathrm{W} - \mathrm{W}_0)}{\rho * \mathrm{V}} * 100\% \quad (3)$$

where W_0 and W are the weight of the sponge before and after immersing in ethanol, respectively, ρ represents the density of absolute ethanol, and V denotes the volume of the sponge [54].

2.3.8. The water vapor transmission rate (WVTR)

The water vapor transmission rate (WVTR) was determined by fixing the sponge (0.2 g) onto the opening of a round plastic box with a diameter of 40 mm, which contained 5 mL of distilled water. The box was placed in an oven at 37 °C for 24 h, and the WVTR was calculated using Formula 4 shown below:

$$WVTR\left(\frac{\frac{g}{m^2}}{h}\right) = \frac{\left(\frac{\Delta w}{\Delta t}\right)}{A} \quad (4)$$

where $\left(\frac{\Delta w}{\Delta t}\right)$ denoted the slope of the plot and A denoted the effective transfer area.

2.4. Antioxidant activity

The DPPH radical scavenging assay was applied to measure the radical scavenging activity of Lev@CBD sponges according to the previously reported method [55]. The main standard compound used was ascorbic acid, which has high antioxidant activity. Briefly, a freshly prepared DPPH reagent (1.0 mM in ethanol) was added to the ascorbic acid and sponges (30 μL), and the reaction was incubated at room temperature for 30 min in the dark. At the end of the incubation time, the absorbance was recorded against a blank at 517 nm using a UV-1800 spectrophotometer (Shimadzu, Japan). The experiment was performed three times. The following Formula 5 calculated the percentage of DPPH radical scavenging:

$$DPPH\ scavening\ (\%) = \frac{(A_0 - A_s)}{A_0} * 100\% \quad (5)$$

where A_0 is the absorbance of the DPPH solution, and A_s is the absorbance of sponge.

2.5. Anti-inflammatory studies

The anti-inflammatory activity of the Lev@CBD sponge was determined by its ability to inhibit bovine serum albumin (BSA) denaturation, as described previously [56]. In brief, 1 mL of 1 mM BSA solution was mixed with 2 mL of the sponge extract. The mixtures were incubated at 37 °C for 15 min, followed by incubation at 70 °C in the water bath for 30 min for denaturation. The absorbance of the obtained blends and the

diclofenac sodium solution was measured at 660 spectrophotometrically at 660 nm. Measurements were performed at different concentrations (10–500 μg/mL). The percentage of inhibition of denaturation was calculated using Formula 6:

$$Inhibition\ (\%) = \frac{(A_s - A_c)}{A_s} * 100\% \quad (6)$$

where, A_0 is the absorbance of the control and A_s is the absorbance of sponge.

2.6. Release of CBD from the obtained Lev@CBD sponges

The release of CBD from obtained materials was measured with the liquid chromatograph Shimadzu Prominence LC (Kyoto, Japan) use. The instrument consists of a quaternary gradient pump (LC-20 CE), an autosampler (SIL—20C), a column thermostat (CTO-10AS), and a spectrophotometric diode-array UV–Vis detector (SPD-M20A). Instrument control, data acquisitions, and data processing were performed with LabSolutions software for HPLC. Chromatographic analyses were performed on the Kinetex C18 column (150 × 4.6 mm) with a particle size of 5 μm using a methanol-water mobile phase in gradient elution at 30 °C. The gradient profile was as follows: initial condition 60 % of MeOH in water, next the increase of MeOH up to 95 % during 4 min. Finally, 95 % of MeOH was maintained to the end of the analysis within 15 min. The detection wavelength was set at 254 nm. Quantitative analysis was performed using the calibration curve. The applied method was linear in the range from 0.8 μg/mL to 1 mg/mL with the coefficient R^2 equal to 0.999.

The obtained levan sponges with a known CBD oil content were placed in Ependorff-type tubes, and methanol (2 mL) was added (the ratio of sponge to methanol was 10:1 *V*/V), which the release experiment was conducted. The samples were incubated in a thermomixer (800 rpm) at room temperature for the specified time (0−12*h*). After an appropriate incubation time, 50 μL of supernatant was collected, transferred to an insert, and placed in an HPLC dispenser. Measurement was performed by taking 10 μL of supernatant. After measurement, the supernatant was returned to the sponge tubes, continuing incubation later.

2.7. Protein adsorption

The adsorption of proteins to the obtained sponge was determined using a fluorescence method. Two types of protein were selected to test the interaction: human serum albumin (HSA) and fibrinogen. First, the solution of HSA (6.24 μM) and fibrinogen (3.78 μM) in PBS (pH = 7.4; 50 mM) was prepared. Then, 0.36 cm^3 of each type of Lev@CBD sponge was immersed in four milliliters of freshly prepared HSA or fibrinogen solution and incubated at a thermomixer (36 °C and 600 rpm). Fluorescence spectra were recorded at various intervals ranging from 290 to 400 nm and 300 to 500 nm for HSA and fibrinogen, respectively, at an excitation wavelength of 280 nm using a Jasco FP-8300 spectrofluorometer (Jasco, Tokyo, Japan). The spectral recording range was 285–500 nm, the scanning speed was 100 nm/min, and the Ex/Em bandwidth was 2.5 nm/5 nm.

2.8. Antibacterial studies

2.8.1. Bacterial cultures

Staphylococcus aureus ATCC 29213 and *Pseudomonas aeruginosa* ATCC 27853 were used in this study. Bacterial strains were stored in Microbank cryogenic vials (ProLabDiagnostics, Canada) at −70 °C ± 10 °C and revived on Tryptic soy agar (TSA). Tested strains were cultured aerobically in Brain Heart Infusion Broth (BHI) at 36 °C ± 1 °C for 18–20 h. Then, microorganisms were harvested by centrifugation (3000 rpm for 15 min), re-suspended in 0.85 % sterile saline solution, and diluted in BHI broth to a final *ca.* 108 CFU/mL concentration.

2.8.2. Time-killing curve assay

Time-kill curve analyses were performed by culturing bacterial strains in BHI broth in the presence of Lev@CBD sponges. For each material and bacterial strain, seven tubes (containing 1 mL of BHI broth) were prepared, and 15 mg of each material sample was added (the amount of sample was set according to the preliminary experiment results). The tubes were pre-incubated for 30 min at 20 °C and inoculated with 10 μL of bacterial inoculum (10^8 CFU/mL). The control growth group was a material-free tube (BHI broth inoculated with bacterial inoculum). A sterility control (medium only) was also included.

At prearranged time points (0, 2 h, 4 h, 8 h, 12 h, and 24 h) after incubation at 36 ± 1 °C, 100 μL of the sample was taken, and the number of viable cells (CFUs/mL) in each sample was determined using standard plate count. The time-killing curves were analyzed by plotting the Log CFU/mL against the time. Experiments were performed in triplicates.

2.9. In vitro biocompatibility testing

L-929 mouse fibroblasts (NCTC clone 929: ECACC No. 88102702) and human dermal fibroblasts (HDF, adult) were purchased from the European Collection of Authenticated Cell Cultures (Salisbury, UK) and used to assess the biocompatibility of the tested biomaterials. The cells were grown in the EMEM medium supplemented with 2 mM L-glutamine, 1 % NEAA, 10 % FBS, and antibiotics (100 U/mL penicillin and 100 μg/mL streptomycin) at 37 °C in a humidified atmosphere with 5 % CO_2. The cell culture was supplemented with the fresh medium twice or thrice a week. Cells in passages 6 to 8 were used in the experiments.

The biological assessment of the prepared biomaterials was performed according to the ISO standard 10993–5, using two different methods (direct contact test and extract test). The direct contact test is performed by placing the test material on a monolayer of fibroblast cells. For the extract test, the material is immersed into the growth medium and the cells are then exposed to the resulting extracts.

Sponges were sterilized with the UV light for 40 min in a laminar flow hood and used for the experiments on the same day. For the 24 h and 72 h extract tests, L-929 and HDF cells were seeded on *96-well plates* at the density of 1×10^4 and 2.5×10^3 of cells per well, respectively, and allowed to grow for 24 h. In the meantime, the biomaterial extracts were prepared by incubating each sponge (formed in a cylindrical shape with a diameter of 6 mm and height of 12 mm, ±1–2 mm) in 4 mL of the growth medium for 24 h at *37 °C in a humidified atmosphere with 5 % CO_2. Then, the medium was replaced with 100* μL *of the extract-containing or extract-free medium (untreated control). In accordance with the ISO standard* 10993–5 recommendations, no *additional processing (e.g., no filtration, centrifugation) was performed on the obtained extracts prior to being applied to the fibroblast cells. For the direct test, 3* × 10^5 cells were seeded per well of 6-well plates and allowed to grow for 24 h. Then, the medium was changed to the *fresh cell culture medium, and one sponge was placed per well and incubated with the cells for 24 h.*

The cytotoxicity of the tested materials was assessed using the MTT assay. At the end of the experiment (24 or 72 h treatment), the medium was removed, and 100 μL or 1 mL of 0.5 mg/mL MTT (Sigma-Aldrich) prepared in the fresh growth medium was added to each well of the 96-well or 6-well plates, respectively. After 3 h of incubation at 37 °C in the CO_2 cell culture incubator, the solution was removed, and 100 μL or 1 mL of 0.04 M HCl-isopropanol was added to each well to dissolve the produced purple formazan crystals. For the direct test, 100 μL aliquots were transferred into 96-well plates. The absorbance was measured at a wavelength of 570 nm with background subtraction at 690 nm using the Synergy HT Multi-Mode Microplate Reader (BioTek Instruments, Winooski, VT, USA). The number of viable cells was calculated relative to the control cells growing in the growth medium without the biomaterial (for the direct test) or its extract (for the extract test). The experiments were performed in three independent experiments ($n > 2$).

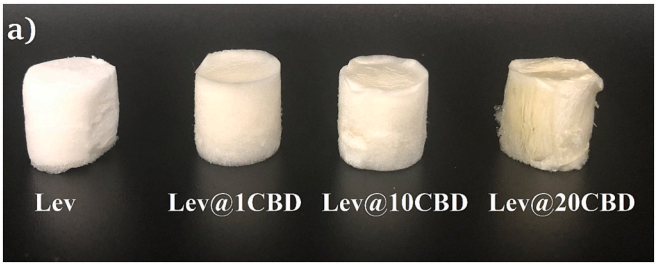

Fig. 1. Photographs of the obtained levan-based sponges (15.5 mm diameter) with different content of cannabis oil – 0 % (Lev), 1 % (Lev@1CBD), 10 % (Lev@10CBD), and 20 % (Lev@20CBD).

2.10. Ex vivo red blood cell hemolysis assay

Whole venous blood from the healthy anonymous human donor was drawn directly to K2-EDTA-coated 10 mL Vacutainer tubes (BD, United Kingdom) to prevent coagulation and processed within 1 h after collection. The whole blood was transferred to centrifugation tubes (Eppendorf, Germany) and centrifuged at 600 ×*g* for 5 min using Eppendorf MiniSpin Plus (Eppendorf, Germany). Levels of hematocrit and plasma were marked on the tube, and plasma was gently aspirated and discarded. The tube was filled to an original plasma level with saline, mixed by gentle inversion several times, and centrifuged at 600 ×*g* for 5 min. Washing was repeated three times. After final washing, saline was removed and replaced with PBS at pH 7.4 (Sigma-Aldrich, Germany), gently mixed, and diluted by PBS (dilution ratio was 1:2.3).

Dried sponge samples (formed in a cylindrical shape with a diameter of 6 mm were immersed in 10 mL of PBS and incubated for 1 h at 37 °C. Supernatants (PBS from tubes with soaked sponges) from all samples were collected and tested for hemolysis along with sponges following the procedure: A) 190 μL of supernatant was transferred into the 96-well plate with U-shaped bottom (GAMA, Czech Republic). In parallel, 190 μL of PBS was used for the negative control (NC), and 190 μL of ultrapure water (prepared with MilliQ IQ 7000; Merck, Germany) was used for the positive control (PC). Erythrocyte suspension (10 μL) was added to each well, and the whole plate was incubated for 1 h at 37 °C; B) Soaked sponges were transferred to 24-well plates (TPP, Switzerland), and 1900 μL of PBS was added to each sample. 1900 μL of PBS or ultrapure water was used for NC and PC, respectively. Subsequently, 100 μL of erythrocyte suspension was added to each well. All samples were gently mixed after 1 h incubation at 37 °C as erythrocytes sunk to the bottom of the plate, and 200 μL of suspension was transferred to U-shaped bottom 96-well plates (GAMA, Czech Republic). U-shaped bottom plates from procedures A) and B) were centrifuged for 5 min at 2000 ×*g* using an Eppendorf 5804R centrifuge (Eppendorf, Germany). The supernatant (100 μL) was carefully transferred to flat-bottom 96-well plates (TPP, Switzerland) without disturbing the erythrocyte pellet, and absorbance was measured at 540 nm using a Tecan Infinite M200 Pro plate reader. The mean value of NC was subtracted from each well. Results (mean ± SD) are expressed as the percentage of PC incubated under the same condition (100 %).

2.11. Evaluation of the stability of Lev@20CBD under constant temperature and relative humidity conditions

The Lev@20CBD sponge was placed in a constant climate chamber for three months (75 % RH, 40 °C) to investigate its activity under constant temperature and humidity conditions. After a time, the sample was taken out, and its non-toxic, anti-inflammatory, and microbiological properties were re-tested. The sponge was studied using the same parameters as the pre-chamber biomaterial tests.

2.12. Statistical analysis

All the obtained data were indicated as the mean ± standard error of the mean. Data were analyzed using one-way analysis of variance (ANOVA) with GraphPad Prism version 6.0 (GraphPad Software, San Diego, CA, USA), followed by Dunnett (to compare every mean to a control mean) or Turkey *post hoc* (to compare every mean with every other mean) test for multiple comparisons. The statistical difference of all the tests was significant, considering $p < 0.05$.

3. Result and discussion

3.1. Characterization of the levan sponges enriched with cannabis oil (Lev@CBD)

Levan is a biocompatible and strongly adhesive polysaccharide with anti-cancer, anti-viral, anti-oxidant, prebiotic, and fibrinolytic properties [30,57–60]. Considering the properties of Lev and its potential to be a good candidate for a material dressing, this work focuses on preparing a levan-based sponge containing cannabis oil (CBD). Our previous work described chitosan films with CBD addition and revealed that the combination of the CBD oil together with the polysaccharide is beneficial [11]. Due to the properties of levan, which may be helpful for use in dressing materials, we decided to obtain new materials in the form of levan-based sponges containing CBD oil. Therefore, in this work, three levan sponges were prepared by setting the mass concentration of CBD oil: Lev@1CBD, Lev@10CBD, and Lev@20CBD (Fig. 1).

The presence of CBD in the materials was confirmed with the ATR-FTIR analysis. Spectra of pure levan and cannabis oil are shown in the Supplementary file (Fig. S1), and spectra of the obtained sponges are demonstrated in Fig. 2. In the spectrum of levan (Fig. S1a), the band at 3003 cm^{-1} corresponds to the O—H stretch of fructofuranose rings, and the peak at 2926 cm^{-1} is attributed to the C—H stretch of fructose rings. Sharp bands at 1123 cm^{-1}, 1014 cm^{-1}, and 925 cm^{-1} are due to the C-O-C symmetric bending vibration of fructofuranose rings and glycosidic linkages [47]. In the spectrum of cannabis oil (Fig. S1b), the band at 3458 cm^{-1} is attributed to the OH stretch of cannabinoids, at 2923 cm^{-1} and 2856 cm^{-1} represent the CH_3 and CH_2 stretching vibrations of the cannabinoids and fatty hydrocarbons. The 1741 cm^{-1} band was assigned to aromatic rings' skeleton vibration, while the band at 1368 cm^{-1} corresponds to CO stretching vibration [61]. For the Lev@CBD sponges, all the characteristic bands of cannabis oil were observed in all samples. Some bands assigned to levan are shifted due to the intermolecular interaction with CBD oil.

The morphology of the Lev@CBD sponges was observed by scanning electron microscopy (Fig. 3). A cross-section of samples is included in Supporting Information (Fig. S6). The surface of the pure levan sponge was smoother with fewer pores and was compact (porosity 33.2 ± 1.8 %). In contrast, all Lev@CBD sponges showed a highly porous structure with interconnected pores (Lev@1CBD, Lev@10CBD, and Lev@20CBD showed porosities of 61.1 ± 2.6 %, 65.8 ± 2.3 %, and 68.4 ± 2.8 %, respectively). This indicates that CBD oil addition promotes the formation of the porous structure without damage or destruction. It might result from the distorted impact of cannabis oil on the internal structure of the polysaccharide. However, increasing the CBD oil amount does not significantly impact the porosity. The increase in the porosity might result from the distorted impact of cannabis oil on the internal structure of the polysaccharide. Moreover, the obtained sponges showed layers with evident lamellar structures comparable to previously applied sponge composites in wound healing with remarkable performances. A high porosity parameter is also beneficial for transferring nutrients and oxygen to the cells attached to the dressings. [62,63]

The thermal properties of biomaterials intended for medical applications constitute crucial factors in evaluating their potential use. Thermal gravimetric analysis was applied to analyze the thermal behavior of Lev@CBD and Lev sponges (the results are shown in Fig. 3e

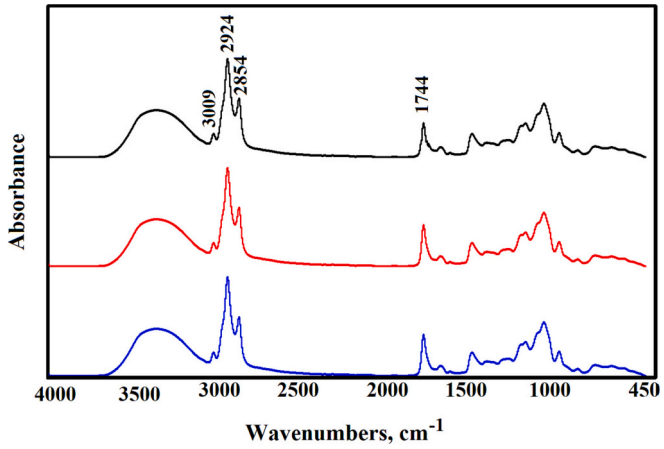

Fig. 2. ATR-FTIR spectra of the obtained Lev@CBD sponges (the black, red, and blue colour corresponds to Lev@1CBD, Lev@10CBD, and Lev@20CBD, respectively) with marked characteristic peaks of cannabis oil. (For interpretation of the references to colour in this figure legend, the reader is referred to the web version of this article.)

and Table S1). For the Lev sponge, two stages of decomposition were observed with gradual loss of weight of the polymer matrix. The first stage, with an initial 9 % weight loss, is due to the polymer's free and bound water loss. The primary decomposition of the Lev sponge started at 190 °C with 67 % weight loss caused by breaking the main chain linkages and bonds in the ring units. These results are well-correlated with the literature data [64–67]. For all Lev@CBD sponges, three clear weight loss steps were observed: the first stage was correlated to the evaporation of adsorbed-bound water, while the second and third steps (from 120 °C to 500 °C), were related to the decomposition of levan and cannabis oil, respectively. Adding CBD oil caused a slight decrease in the thermal stability of all sponges compared to pure levan. The most significant decrease was observed for the sample with the highest cannabis oil concentration. Moreover, at temperatures above 600 °C, no changes in TG and DTG curves were observed, which allows concluding that a rigid and thermally stable structure was obtained as was previously reported, *e.g.*, for the SA/PVA hydrogels containing *Aloe vera* [68].

The mechanical properties of wound dressings play an essential role in wound healing by providing a barrier against infection and maintaining their integrity during application and wearing [69]. This study used tensile strength, stress-strain curves (Fig. 4a), and Young's modulus (Table S2) to assess the sponges' mechanical properties. The sponges' tensile strength was about 3.06–7.04 MPa, consistent with the results presented in other works [70,71]. The Young's modulus of Lev@1CBD, Lev@10CBD, and Lev@20CBD was 95.62 ± 0.13 MPa, 145.54 ± 0.96 MPa, and 199.43 ± 0.87 MPa, respectively (Table S2). This parameter is significantly increased compared to Lev with 60.23 ± 0.26 MPa. Adding CBD oil to the composition of the Lev sponge caused an increase in stress-at-break and maximal elongation-at-break values. Moreover, these values gradually increased as the concentration of the oil increased. The best tensile strength and elongation at break were obtained for the Lev@20CBD sponge (7.04 ± 0.17 MPa and 8.76 ± 0.21 %, respectively), indicating that this sponge could fit well with skin tissue as dressing materials in the most elastic areas. Generally, the tensile strength of healthy human skin ranges from 2.5 to 35 MPa, while Young's modulus ranges from 4.6 to 20 MPa [72]. The mechanical properties of the designed dressings should be better than that of healthy skin so that the wound dressing material does not damage even when the wound is slightly moved. The results for the sponges suggest that the designed materials show good mechanical properties and could be used as dressings.

Adhesion properties also constitute an essential factor related to the potential applicability of materials in medicine. It is because adverse effects on wound healing can be reduced during dressing changes. Inaccurate application of dressings during wound healing can lead to adventive acts and prolonged destruction of proliferating cells [73]. Therefore, the adhesive strength of the obtained sponges was measured. As shown in Fig. 4b, the adhesion forces for all samples were between 2 and 3 N. Addition of CBD oil slightly affected the adhesion strength of the samples. Lev@20CBD sponge showed the highest adhesion force, which may have implications for the cytotoxicity testing of samples. These results relating to the mechanical and adhesive properties of Lev@CBD sponges indicate that they meet the requirements of repetitive stretching and good adhesion for real-use material dressing. The adhesion force may be relatively low for healthy human skin but still sufficient to maintain skin contact with various material surfaces. However, the adhesive strength of intact skin has a different value because it is a complex process that depends on many variables. A wound dressing that is too non-adherent may cause skin damage when removed, while a wound dressing with too little adhesion may not stay in place and perform its function [74].

The swelling percentage represents the degree of hydrophilicity of the material. The swelling capacity of dressings is crucial for hemostasis and wound healing further down the line by regulating bleeding, drugs' release, degradation, and biological fluid absorption [75]. Because the wound healing process involves pH changes, *i.e.*, pH = 7 in the wounded tissue and pH = 5–6.8 in the healed skin tissue, the sponges' swelling characteristics were analyzed at both pH values (Fig. 4c) up to 24 h. The results reflect that all samples showed rapid swelling in PBS solution at both pH values. However, the swelling rate of the prepared sponges was higher at the pH of 7.4 than at pH 5.5. These results are consistent with literature reports [76,77]. As the concentration of CBD oil increased from 1 % to 10 % or 20 %, the swelling rate increased; however, the difference in the swelling rate for concentrations of 10 % and 20 % cannabis oil is minimal. This increase in swelling might be due to the presence of hydrophilic OH groups in the chemical structure of cannabidiol. When the sponge is immersed in an aqueous media polymeric group, it undergoes ion exchange with water molecules in as much as these hydroxyl groups repel each other, therefore decreasing the polymeric chain's entanglement [78]. Also, other authors have described the swelling rate as increasing with a higher concentration of a plant extract [79,80]. These results indicate that all levan sponges with cannabis oil have good swelling behavior, which could promote skin wound healing.

An essential feature of wound dressings is their biodegradability, which indirectly affects the functioning of cells. The dressings need good degradability to prevent secondary wound injury after wound hemostasis [81,82]. Therefore, the sponges' biodegradation profile at different time intervals was analyzed, and the results are shown in Fig. 4d. It can be seen that all Lev@CBD sponges showed a faster degradation profile than the Lev sponge. The biodegradation ratio of the Lev sponge in 14 days was 73.66 ± 0.25 %, and the degradation rates of Lev@1CBD, Lev@10CBD, and Lev@20CBD were 76 ± 0.11 %, 83.7 ± 0.11 %, and 86.7 ± 0.23 %, respectively ($p < 0.05$). Moreover, the biodegradation ratio increased with the higher concentration of oil. This is probably due to the introduction of CBD oil, probably due to the increased solubility, and finally, the decomposition rate of Lev@CBD sponges.

The wound dressing with optimal water vapor transmission rate (WVTR) prevents dehydration from the wound bed and creates an environment with an ideal moisture level for wound healing. Moreover, it also promotes angiogenesis, tissue epithelialization, and clearance of dead tissue. The WVTR of normal skin is 204 g/m^2/day; however, for injured skin, it might range from 279 g/m^2/day to 5138 g/m^2/day. It is considered that an ideal wound dressing should demonstrate the WVTR range of 2000–2500 g/m^2/day to allow wound healing [78,83]. The vapor transmission rate of the Lev sponge was determined to be 2021.3 ± 1.9 g/m^2/day, indicative of a high vapor transmission rate. Incorporating the cannabis oil caused a slight increase of the WVTR parameter

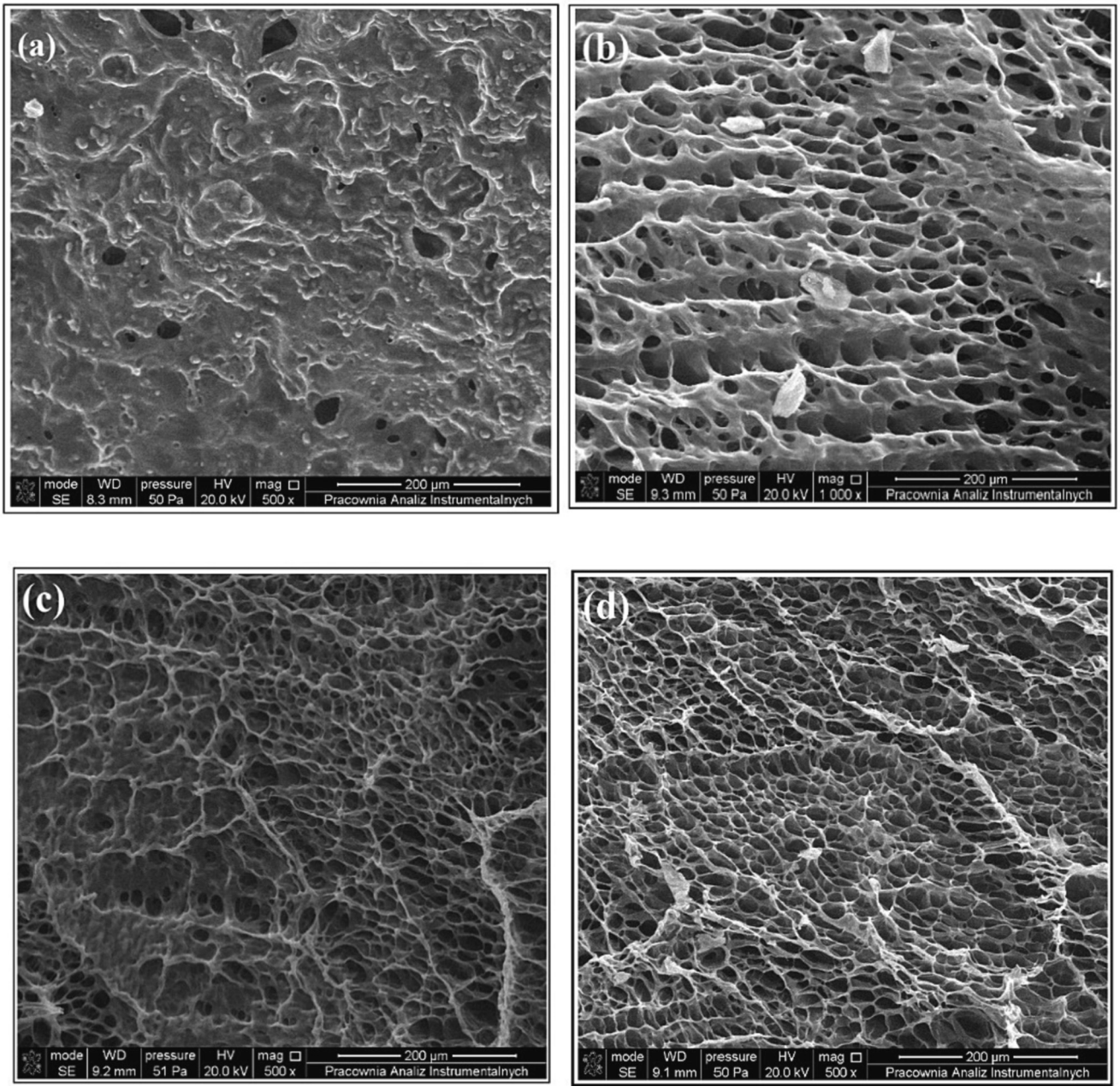

Fig. 3. SEM images of (a) Lev, (b) Lev@1CBD, (c) Lev@10CBD, and (d) Lev@20CBD sponges, e) thermal analysis of the obtained sponges.

to 2044.7 ± 2.6 g/m^2/day, 2060.1 ± 2.3 g/m^2/day, and 2081.6 ± 4.4 g/m^2/day for Lev@1CBD, Lev@10CBD, and Lev@20CBD sponges, respectively. The rise in WVTR is probably related to the interaction of the CBD oil components with the polymer chain, increasing the interaction between the matrix and the plant extract. This phenomenon was confirmed by the literatur e [84,85]. The results show that all prepared sponges are well permeable to water vapors and capable of maintaining an optimal moist environment at the wound site without excessive dehydration.

3.2. Antioxidant activity

During wound healing, the free radicals at the wound site impede healing through enzyme inactivation, lipid peroxidation, and DNA damage caused by oxidative stress. The substances with superior free radical scavenging properties stimulated the wound healing process [86]. Therefore, the antioxidant ability of the Lev@CBD sponges was assessed by the DPPH• scavenging test, considered a standard method. The obtained results are shown in Fig. 5a. It is well-known that levan exhibits antioxidant properties [87,88]. The common antioxidant vitamin, ascorbic acid, showed 90.83 % ± 11.15 activity at 500 µg/mL, whereas the levan exhibited 68.93 % ± 2.2 antioxidant activity at the same concentration ($p < 0.05$). However, the introduction of cannabis oil into the structure of the Lev sponges caused an enhancement of their antioxidant properties. As the concentration of CBD oil increases, the scavenging activity also increases, which is related to the oil's antioxidant properties. Overall, the Lev@CBD sponges with good antioxidant ability show great potential as wound dressing.

3.3. Anti-inflammatory studies

Inflammation has been implicated as an essential response in wound healing mechanisms aimed at renovating and preserving the cellular structure and functional integration in affected tissue segments [89].

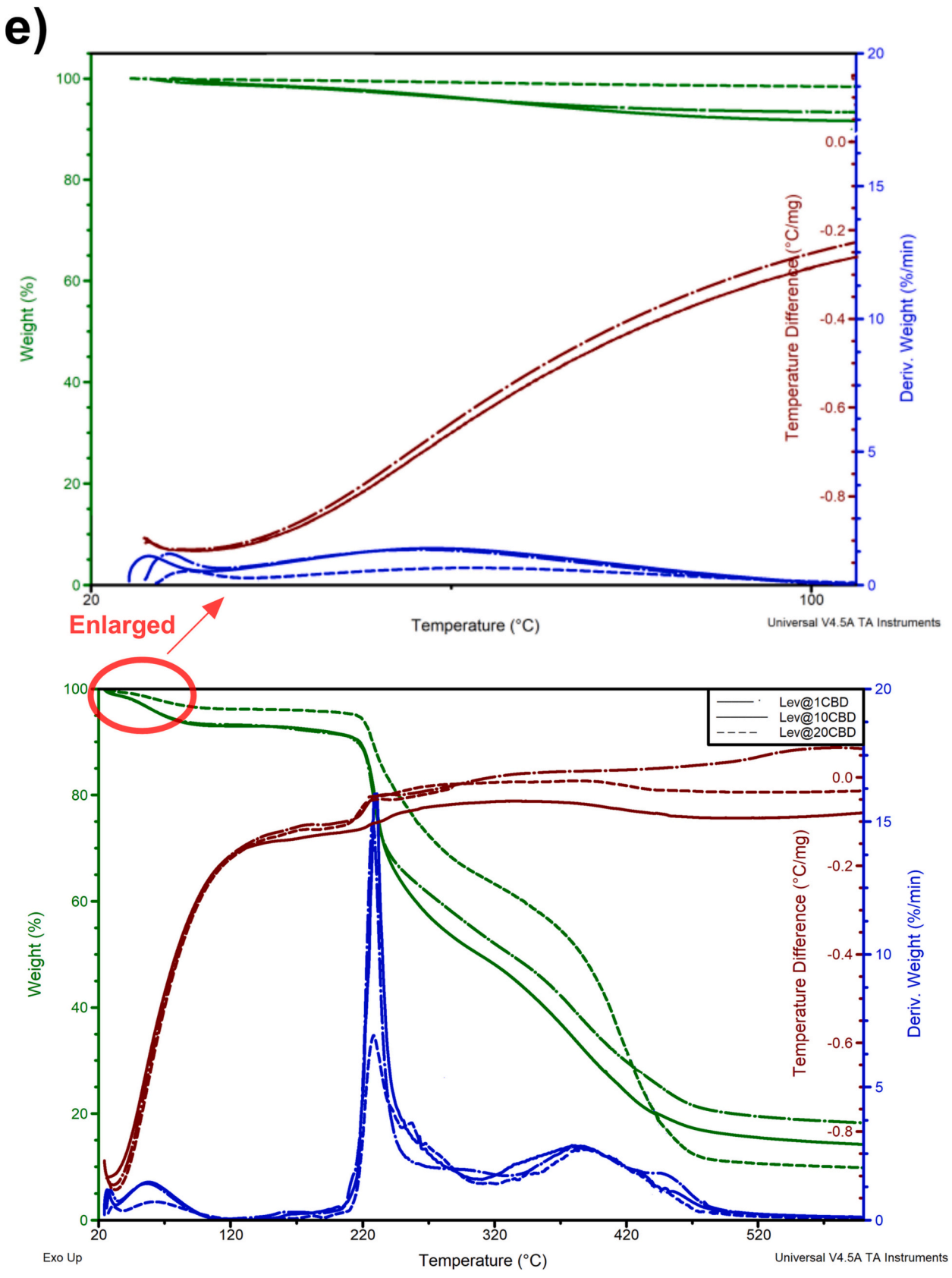

Fig. 3. (*continued*).

The anti-inflammatory assay was estimated using the bovine serum albumin (BSA) denaturation method, and the results are shown in Fig. 5b. The standard NSAID drug diclofenac sodium salt showed 100 % anti-inflammatory activity at the concentration of 400 and 500 μg/mL, and the levan showed 48.17 % ± 14.43 anti-inflammatory activity at the same concentration. Similar results have been obtained in other works

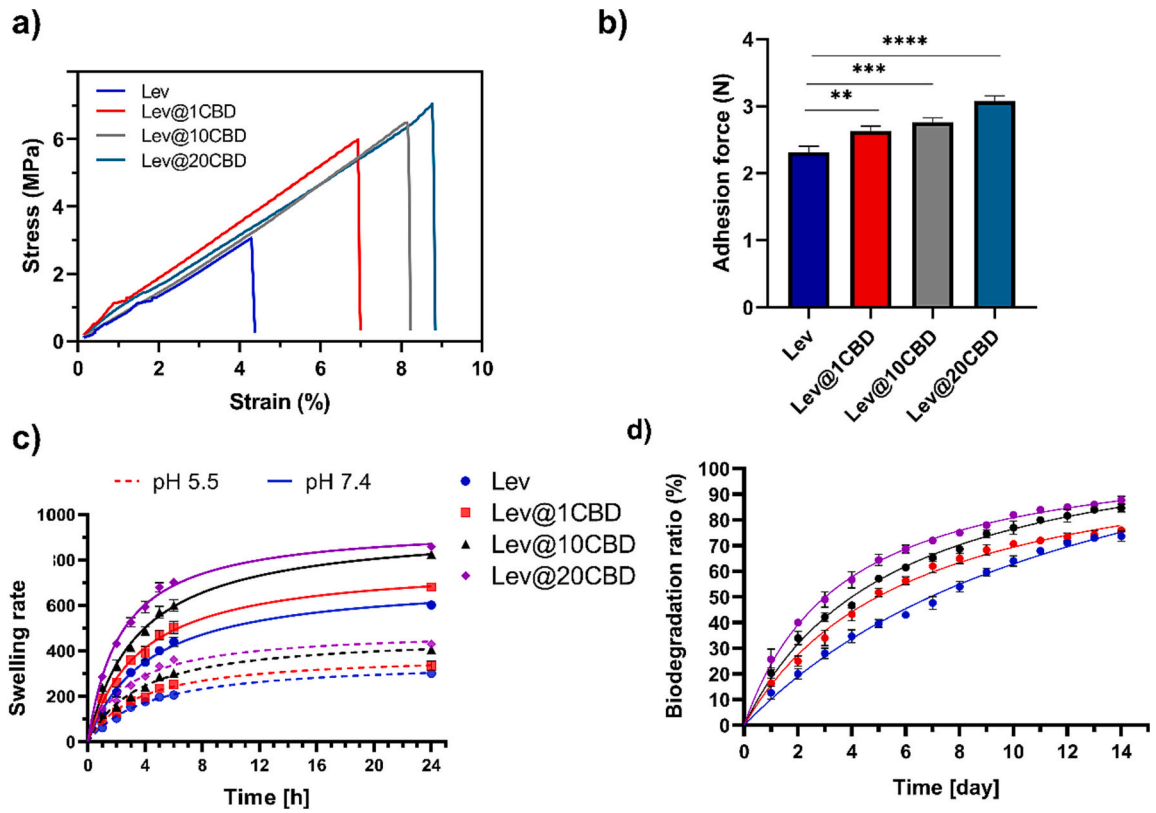

Fig. 4. Mechanical properties of the obtained sponges measurements: a) Stress and strain curve, b) adhesion force of Lev and Lev@CBD showing increasing adhesive strength with increasing content of cannabis oil in the sponges; c) swelling characteristics at pH 5.5 and pH 7.4 (PBS, 37 °C) d) degradation profile (PBS containing lysozyme, 37 °C); $^{**}p < 0.01$, $^{***}p < 0.001$.

[57,90], confirming that pure Lev exhibits anti-inflammatory properties. However, our studies proved that cannabis oil also has these properties, as demonstrated by the results obtained for the Lev@CBD sponges. All sponges with CBD oil exhibit strong anti-inflammatory activity. Moreover, as the CBD oil concentration increased, the inhibition of the BSA denaturation of the samples also increased. This study revealed that CBD oil enhances the anti-inflammatory properties of the Lev@CBD sponges; hence, they might be used as wound dressing material with intense anti-inflammatory activity.

3.4. Release of CBD from the obtained Lev@CBD sponges

The action mechanism of potential wound dressing materials is related to releasing the embedded substances into the surrounding space. Therefore, the prepared sponges' antimicrobial, antioxidant, and anti-inflammatory efficiencies are strictly correlated with the release of the oil. To this purpose, we studied the release of CBD loaded in levan sponges over 24 h *via* the HPLC method. Results show that all the obtained sponges with cannabis oil released up to 12.73 % bioactive substances in 24 h (Fig. 5c). In our post-previous work [11], up to 13 % CBD was released from the chitosan matrix, indicating that cannabis oil releases similarly regardless of the type of matrix used. The data analysis exposed a slow release of CBD from the Lev@CBDs. This slow release exposes the potential of the resulting biomaterials to where drug release is required over an extended time [91]. Lev@10CBD and Lev@20CBD samples showed a slight difference in the release of active substances (12.26 % and 12.72 %, respectively). This is related to the swelling rate of these sponges, the value of which also showed a slight difference (858.67 % and 826.67 %, respectively). The increase in the amount of substance released may also be the result of increased diffusion of CBD, which is present on the surface of the sponges [92]. Regarding the results, levan sponges incorporated with cannabis oil could be active for up to 24 h.

3.5. Protein adsorption

Protein adsorption constitutes an essential physical property for wound dressings. Wound exudate, which contains many proteins, must be absorbed to promote wound healing [93,94]. Albumin is the most abundant protein in blood plasma. It is also one of the crucial proteins to bind xenobiotics [67,95]. Therefore, it is essential to understand how the properties of the newly designed biomaterial affect the amount of adsorbed albumin and how they may affect the succeeding immunological response. Another important protein is fibrinogen (FB), which is considered to be a vital glycoprotein that is significantly related to blood coagulation and further scar formation [96,97]. Therefore, we used both proteins HSA and FB to determine the protein adsorption of Lev@CBDs. The amount of bound proteins with the sponges was determined after different incubation times (1 min - 24 h). Fig. 6 shows the results for the selected incubation time, while the entire time range is given in Table S3 and Fig. S2. As shown in Fig. 6, all the obtained biomaterials can adsorb both proteins, and the amounts of bounded proteins increased suddenly after 24 h for Lev@CBDs compared to pure levan. Moreover, the protein adsorption capacity increased with increasing CBD oil concentration. Lev@1CBD sponge showed the lowest adsorption of both proteins, while Lev@20CBD showed the highest adsorption of HSA and FB of about 4.3 mg/cm^2 and 10.8 mg/cm^2, respectively, at the time of 24 h. The increased amount of adsorbed HSA and FB could also be related to increased sponges' porosity. The results demonstrate that the adsorption capacity of FB is much better than that of HSA, which can be attributed to the increased procoagulant capability of Lev@CBD [98,99]. It is also considered that a higher amount of proteins adsorbed on biomaterials

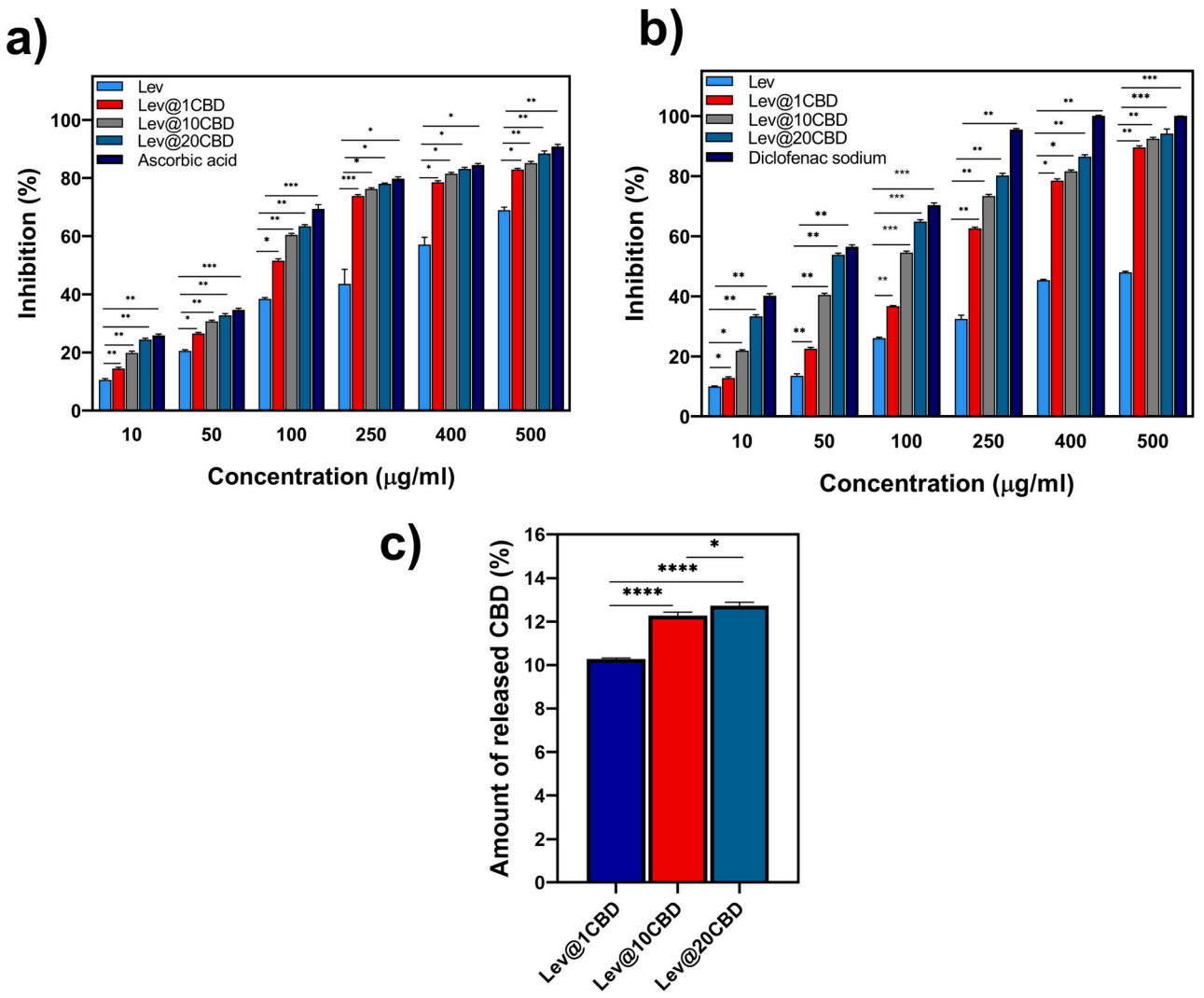

Fig. 5. The Lev@CBD sponges' characteristics: (a) Antioxidant, (b) anti-inflammatory activity, and c) release of CBD from the sponges; *$p < 0.05$, **$p < 0.01$, ***$p < 0.001$.

can provide more significant attachment sites for cells and help improve cell adhesion [100]. Therefore, the sponge with the highest CBD concentration showed the most biocompatibility.

3.6. Antibacterial studies

In the antimicrobial studies, the activity of Lev, Lev@1CBD, Lev@10CBD, and Lev@20CBD against representatives of Gram-positive cocci – *Staphylococcus aureus* ATCC 29213 and Gram-negative rods – *Pseudomonas aeruginosa* ATCC 27853 were performed. *S. aureus* and *P. aeruginosa* are the most prominent causes of acute and chronic wound infections [101–103]. A high ability to produce numerous virulence factors and biofilm formation, as well as the intrinsic resistance to many antimicrobials, make *S. aureus,* especially *P. aeruginosa* infections,

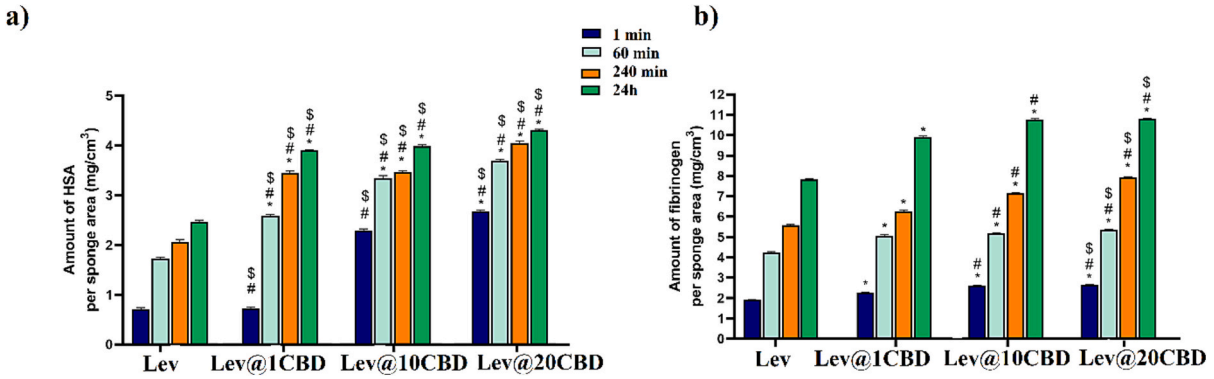

Fig. 6. Amount of bounded a) HSA and b) fibrinogen at the surface of the obtained sponges. *, #, $ indicate $p < 0.05$ when compared to the Lev, Lev@1CBD, and Lev@10CBD, respectively.

extremely difficult to treat [104]. In addition, these microorganisms can acquire resistance mechanisms to various antimicrobials, and currently, many infections are caused by multi-drug resistant strains (MDR), resulting in therapeutic failures. Therefore, the search for alternative or complementary antibiotic treatments should be a priority for modern medicine.

In this study, the formulations were tested in time-kill curve studies to determine the antibacterial effect and its dependence on concentration over time, with results summarized in Fig. 7. For Lev, an inhibition was noted against *S. aureus* for up to 12 h (Fig. 7a), but in the subsequent hours of incubation, the Lev inhibitory effect was not further observed. After 24 h, the number of isolated microorganisms was similar to that of microorganisms isolated from the control sample without sponges. Adding CBD oil to Lev sponges significantly increased its antibacterial effect, and Lev@1CBD, Lev@10CBD, and Lev@20CBD showed a concentration-dependent increase in activity against *S. aureus*. According to the Clinical and Laboratory Standards Institute (CLSI), *significant bactericidal activity* is defined as a reduction in the bacterial cells by 3 logs compared to the initial inoculum [105]. In the case of formulations Lev@1CBD and Lev@10CBD, the highest reduction in the number of microorganisms, close to 3 logs, was obtained after 8 h of incubation. The most effective *S. aureus* inhibition was achieved for Lev@20CBD. A significant reduction of >3 logs (from 6.3 to 2.6 log10 CFU/mL) in microbial counts (bactericidal effect) compared with the starting inoculum was observed after 8 h of *S. aureus* incubation with Lev@20CBD. It is worth noting that the significant inhibition (bacteriostatic effect) was observed at all concentrations of CBD even after 24 h of incubation compared to the initial bacterial inoculum (from 6.3 to approx. 5 log10 CFU/mL), which means that the growth of about 90 % of the bacteria was inhibited.

The antibacterial effect of tested formulations against P. aeruginosa was recorded only during the first 4 h of incubation (Fig. 7b). However, the trend towards greater potency upon the complexation of Lev was not observed. In contrast to S. aureus, a regrowth caused by the loss of antibacterial properties was observed already after 8 h of incubation for all formulations. The differences in the bacterial count between the formulations were generally slight. However, the number of isolated microorganisms from samples containing Lev, Lev@1CBD, Lev@10CBD, and Lev@20CBD was lower than for the control.

The kinetic profiles of tested formulations exhibited bacteriostatic or even bactericidal activities against *S. aureus*. Growth inhibition of Gram-negative bacteria was observed only during the first 4 h, with subsequent regrowth of *P. aeruginosa* nearly to the untreated control values (no sponges). The greater antimicrobial efficacy of tested formulations observed towards *S. aureus* than *P. aeruginosa* could be attributed mainly to the differences in cell structure between Gram-positive and Gram-negative bacteria. The cell wall of Gram-negative bacteria is more complex due to the presence of an additional outer membrane covering the surface of the peptidoglycan. This remarkable structure protects the cell from adverse physical and chemical factors and makes Gram-negative bacteria less sensitive to many antimicrobials [106].

Based on these data, the tested Lev@CBD sponges possess antibacterial potency. They might be suitable candidates for wound dressing, presenting a good starting point for further study to evaluate the mechanism of action to strengthen their bactericidal potential.

3.7. In vitro biocompatibility testing

An ideal wound dressing should exhibit low cytotoxicity and, therefore, biocompatibility, especially with skin fibroblasts. Two cell lines were used to evaluate the cytotoxic properties of the sponges: L929 mouse fibroblasts and normal human dermal fibroblasts (HDF). According to ISO standard 10,993–5, two different culture methods were used: direct contact and extract assays. The cell viability of L929 and HDF cells was examined after 24 h (Fig. 7c,d) and 72 h (Fig. S5) incubation directly with the samples and their extracts. After 24 h, only Lev (pure levan sponge) extract showed a slightly toxic effect against L929 cells (cell viability around 80 % of untreated control), while the viability of HDF cells was above 90 % (Fig. 7c). These results correspond well with literature reports [107–109]. Adding cannabis oil increased the cell viability of both cell lines treated with extracts in all cases (100–120 %) compared to untreated control, with the best results obtained for the levan sponge containing the highest concentration of CBD oil (*i.e.*, Lev@20CBD). Interestingly, the viability of L929 fibroblasts cultured in Lev and Lev@1CBD extracts for 72 h decreased slightly, while Lev@20CBD increased the cell viability by approximately 30 % compared to the control cells. This suggests that this sample has beneficial long-term effects. In contrast, the cytotoxicity of Lev@20CBD extract with the HDF did not change (Fig. S5a).

L929 and HDF cells were also cultured directly with the obtained sponges (Fig. 7d). This method allowed to detect slight cell viability decrease only for Lev (formulation without cannabis oil) and Lev@1CBD. On the other hand, this decrease was only to 90 % and 88 % on L929 and HDF, respectively, for Lev, and 95 % and 92 % on L929 and HDF, respectively, for Lev@1CBD. Compared to untreated control, formulations with higher concentrations of cannabis oil either didn't significantly change cellular viability or slightly increased viability (up to 105 % and 104 % for Lev@20CBD on L929 and HDF cells, respectively). Results on both cell types were similar for the respective samples, confirming the non-toxicity of the biomaterials.

Another biocompatibility aspect that needed to be considered was the inability of studied materials to induce damage to erythrocytes – therefore, the inability of hemolysis – as sponges might possibly get into direct contact with blood from compromised blood vessels in the wounds. Moreover, compounds released from sponges can enter the bloodstream therein, causing hemolysis there. Hence, the *ex vivo* hemolysis assay was performed directly with sponges and extracts, similar to the fibroblast experiments. All levan sponges containing cannabis oil didn't cause any hemolysis, and the results were, therefore, comparable with untreated erythrocytes (Fig. 7e). The biocompatibility results showed that all the obtained sponges did not have cytotoxicity.

3.8. Evaluation of Lev@20CBD stability under constant temperature and relative humidity conditions

Suitable dressing materials should maintain their crucial properties under different conditions. The study presented in this work showed that the Lev@20CBD sponge has more beneficial properties than the others (including biocompatibility test, anti-inflammatory, and antibacterial properties). Therefore, this sample was selected for testing its behavior under constant temperature and relative humidity conditions. Lev@20CBD was placed for three months in a climate chamber that complies with the ICH guidelines for stability testing of pharmaceutically active substances at 40 °C and 75 % RH [110]. After a time, the sponge was removed from the air chamber, and its biological activity was re-studied.

The microbiological test results are shown in Fig. 8a. The time-kill kinetic assays of Lev@20CBD subjected to the aging process exhibited stronger antimicrobial activity against both *S. aureus* and *P. aeruginosa* than an unaged sponge. Significant bactericidal activity towards *S. aureus* was observed after eight hours of exposure. During incubation, the number of isolated bacterial cells decreased from 6.3 logs to 1.5 logs (compared to 2.6 log10 CFU/mL for an unaged sponge). Although the number of CFUs in the sample increased in longer incubations, it was still approx. 2 logs lower than the initial inoculum value. Therefore, the bacteriostatic effect analogical to the unaged sponges was maintained.

For *P. aeruginosa,* a reduction consistent with the inhibition effect was observed over 12 h (a decrease in the number of bacterial cells from 5.9 logs to 4.0 logs after four hours and 4.3 logs after 12 h). An increase in bacterial counts (7.63 logs) almost to the untreated control value (9.3 logs) was noted after 24 h of exposure.

The process of aging test material at constant temperature and

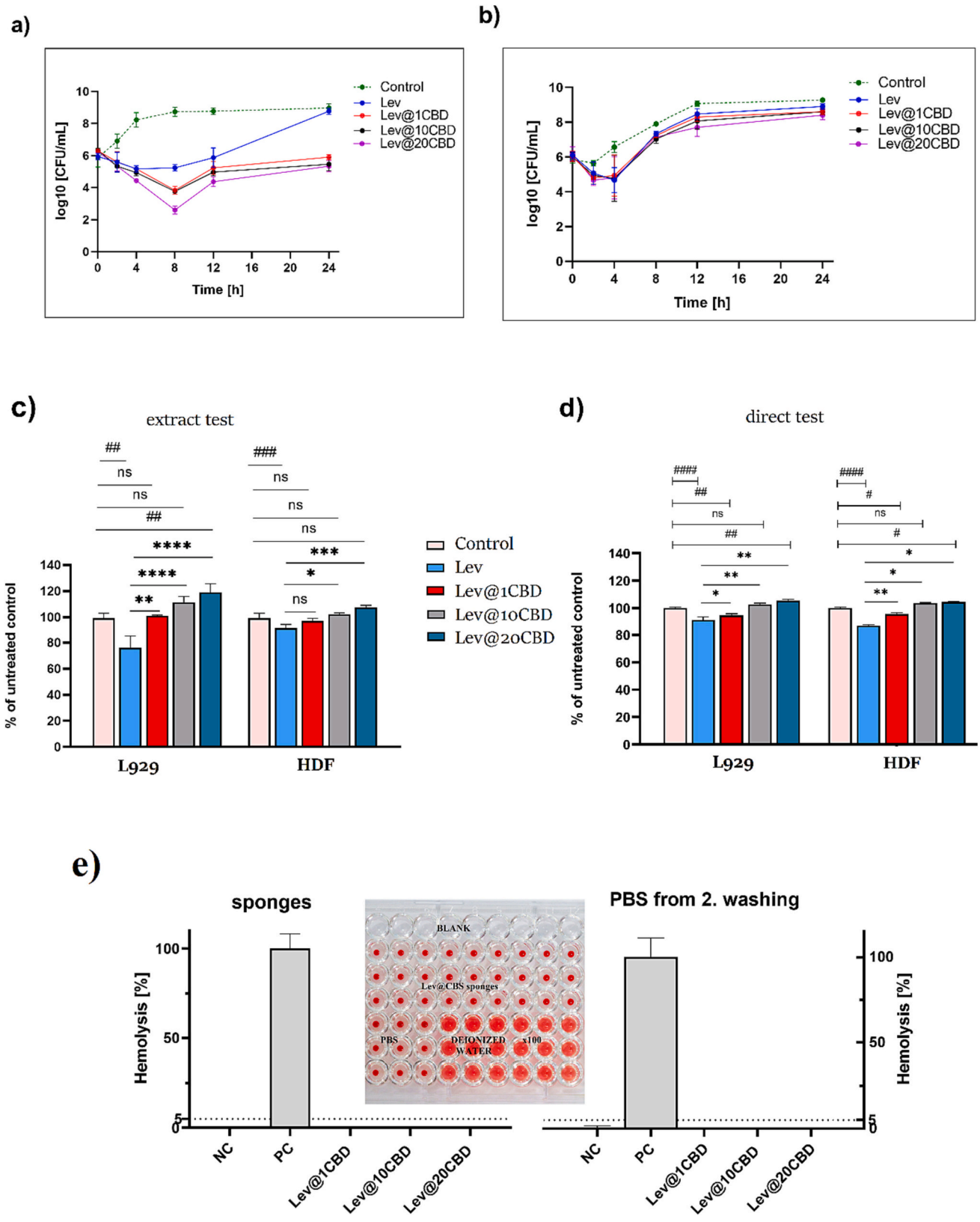

Fig. 7. Biological properties of the sponges. Time-killing curves of a) *S. aureus* and b) *P. aeruginosa* in the presence of the studied biomaterials. Cell viability of L929 and HDF cells after 24 h incubation c) with 100 % extracts obtained from tested sponges. # and * show statistical significance compared to untreated control and Lev, respectively d) in direct contact with sponges, and e) *ex vivo* red blood cell hemolysis assay on the prepared sponges; NC – negative control (untreated erythrocytes); PC – positive control (erythrocytes treated with x100). (For interpretation of the references to colour in this figure legend, the reader is referred to the web version of this article.)

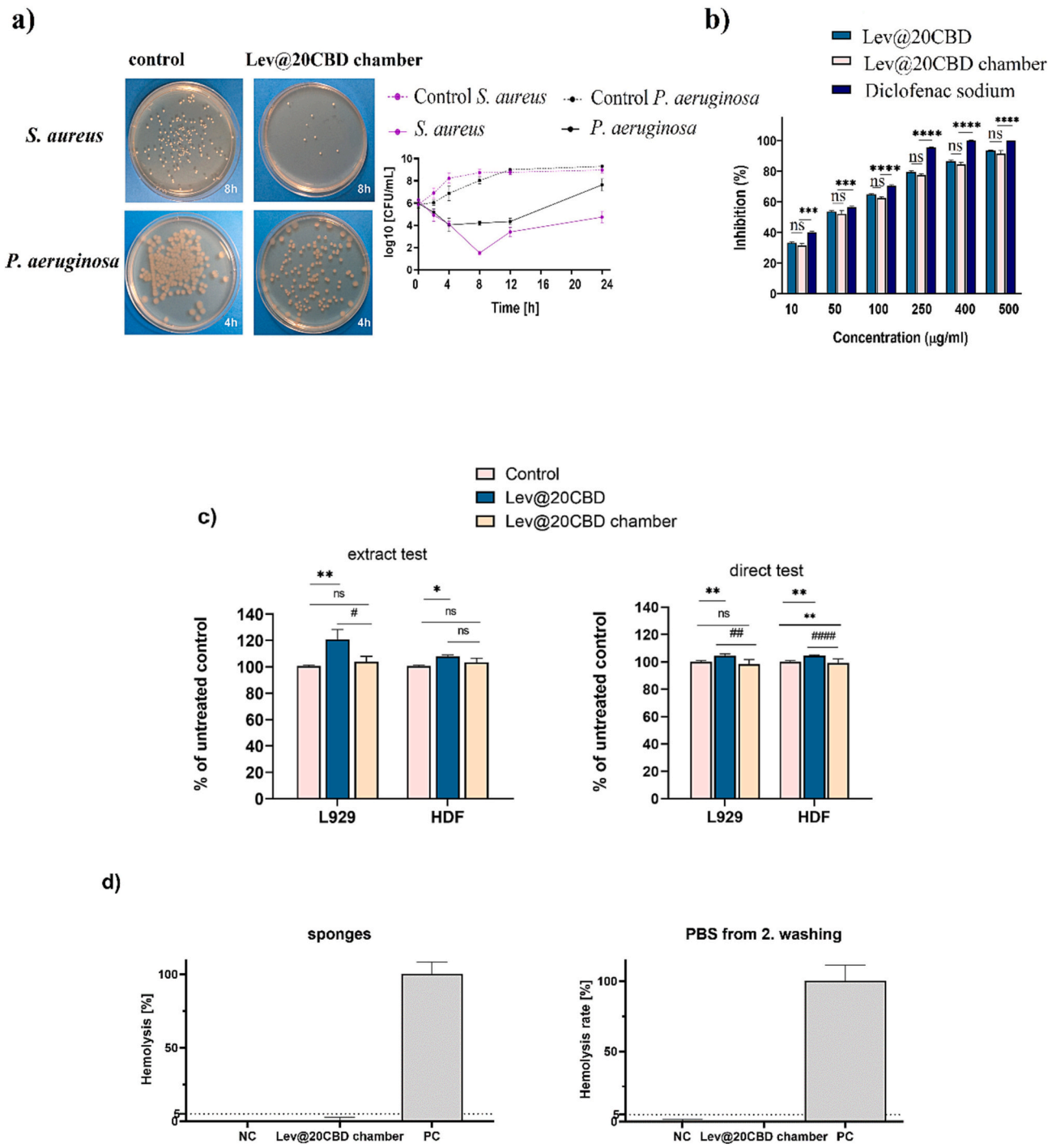

Fig. 8. Properties of Lev@20CBD sponge subjected to constant relative humidity (75 %) and increased temperature (40 °C) for three months. a) Time-killing curve of *S. aureus* and *P. aeruginosa* in the presence of the obtained biomaterials, b) anti-inflammatory properties; c) the viability of L929 and HDF cells after 24 h incubation, d) *ex vivo* red blood cell hemolysis assay. (For interpretation of the references to colour in this figure legend, the reader is referred to the web version of this article.)

humidity changes the morphology of the resulting sponges. It might result in better contact between the active substances and bacteria and, consequently, their faster killing in the microbiological test.

The Lev@20CBD sponge, subjected to constant relative humidity and temperature, still showed strong anti-inflammatory properties (Fig. 8b). It can be observed that the anti-inflammatory activity decreased slightly compared to the initial sample, but this decrease was statistically insignificant. At the highest concentration (500µg/mL), the Lev@20CBD sponge still behaves similarly to the standard diclofenac sodium (a reduction from 93.53 % to 91.43 % compared to the starting sponge). It means the designed biomaterial could be used in areas with harsh conditions of constant temperature and relative humidity.

Cytotoxicity studies showed that storing the sample for three months under constant temperature and relative humidity had no significant effect on cell viability after 24 h incubation with L929 and HDF fibroblasts. The Lev@20CBD extract and its direct contact (Fig. 8c) with fibroblasts showed a slight decrease in cell viability, but the sample didn't display acute toxicity. The most significant changes were observed after 72 h treatment of the extract with HDF (Fig. S5b). In this case, the viability dropped to 56 % compared to the control, showing possible

cytotoxicity upon prolonged exposure to aged material. Note that no toxicity was detected with fresh unaged material. These results suggest that the sample can be used for 24 h even after three-month exposure to harsh conditions without showing a cytotoxic effect. Moreover, the material is still non-hemolytic, as shown in Fig. 8d.

4. Conclusions

The biomaterials consisting of levan sponges enriched with cannabis oil are expected to be suitable wound dressing due to their highly effective characteristics, as discussed in this article. Specifically, a competent group of advantages (porous structure, good mechanical, antioxidant, anti-inflammatory, and antimicrobial properties, a high swelling ratio in different pH, and well biodegradation profile) renders the sponges to be an appropriate solution for treating damaged tissue. *In vitro* biocompatibility studies confirmed that the prepared sponges were non-toxic towards L929 and HDF cells. Moreover, the obtained biomaterials can interact with essential proteins in wound healing. Most significantly, the biomaterials retained their non-hemolytic, anti-inflammatory, and antimicrobial properties after storage in a climate chamber at a constant temperature and relative humidity. The results from the release of CBD indicated that the obtained sponges could be active for up to 24 h. Overall, these results showed that prepared sponges enriched with cannabis oil might have significant potential for applications in wound healing, tissue engineering, and cell culture.

CRediT authorship contribution statement

Dorota Chelminiak-Dudkiewicz: Conceptualization, Investigation, Collected the data, Interpretation of data, wrote the original paper. Miloslav Machacek and Jolanta Dlugaszewska: Investigation, partial interpretation of data. Magdalena Wujak, Aleksander Smolarkiewicz-Wyczachowski, Kinga Mylkie, Szymon Bocian, Michal P. Marszall, and Tomasz Gośliński: Investigation. Marta Ziegler-Borowska: revised the paper, supervising.

Declaration of competing interest

The authors declare that they have no known competing financial interests or personal relationships that could have appeared to influence the work reported in this paper.

Data availability

Data will be made available on request.

Acknowledgment

The Authors thank Jolanta Wolkiewicz and Artur Borowski for their technical support.

This work was supported by the National Science Centre Poland grant UMO-2022/47/D/NZ7/01821.

D.Ch-D., M.W., A. S—W., K.M., M.P.M., and M.*Z*-B. are members of the Center of Excellence, Towards Personalized Medicine" operating under Excellence Initiative – Research University.

Parts of the paper were checked in terms of grammar and language with the assistance of DeepL and Grammarly.

Appendix A. Supplementary data

Supplementary data to this article can be found online at https://doi.org/10.1016/j.ijbiomac.2023.126933.

References

[1] M. Naseri-Nosar, Z.M. Ziora, Wound dressings from naturally-occurring polymers: a review on homopolysaccharide-based composites, Carbohydr. Polym. 189 (2018) 379–398.
[2] M. Parani, G. Lokhande, A. Singh, A.K. Gaharwar, Engineered nanomaterials for infection control and healing acute and chronic wounds, ACS Appl. Mater. Interfaces 8 (16) (2016) 10049–10069.
[3] S. Anbazhagan, K.P. Thangavelu, Application of tetracycline hydrochloride loaded-fungal chitosan and Aloe vera extract based composite sponges for wound dressing, J. Adv. Res. 14 (2018) 63–71.
[4] S. Ye, L. Jiang, J. Wu, C. Su, C. Huang, X. Liu, W. Shao, Flexible amoxicillin-grafted bacterial cellulose sponges for wound dressing: in vitro and in vivo evaluation, ACS Appl. Mater. Interfaces 10 (6) (2018) 5862–5870.
[5] S. Farzamfar, M. Naseri-Nosar, H. Samadian, S. Mahakizadeh, R. Tajerian, M. Rahmati, A. Vaez, M. Salehi, Taurine-loaded poly (ε-caprolactone)/gelatin electrospun mat as a potential wound dressing material: in vitro and in vivo evaluation, J. Bioact. Compat. Polym. 33 (3) (2017) 282–294.
[6] E. Rezvani Ghomi, S. Khalili, S. Nouri Khorasani, R. Esmaeely Neisiany, S. Ramakrishna, Wound dressings: current advances and future directions, J. Appl. Polym. Sci. 136 (27) (2019) 47738.
[7] J. Su, J. Li, J. Liang, K. Zhang, J. Li, Hydrogel preparation methods and biomaterials for wound dressing, Life 11 (10) (2021) 1016.
[8] V.d.A.M. Gonzaga, A.L. Poli, J.S. Gabriel, D.Y. Tezuka, T.A. Valdes, A. Leitão, C. F. Rodero, T.M. Bauab, M. Chorilli, C.C. Schmitt, Chitosan-laponite nanocomposite scaffolds for wound dressing application, J. Biomed. Mater. Res. B Appl. Biomater. 108 (4) (2020) 1388–1397.
[9] H. Türe, Characterization of hydroxyapatite-containing alginate-gelatin composite films as a potential wound dressing, Int. J. Biol. Macromol. 123 (2019) 878–888.
[10] A. Shahzad, A. Khan, Z. Afzal, M.F. Umer, J. Khan, G.M. Khan, Formulation development and characterization of cefazolin nanoparticles-loaded cross-linked films of sodium alginate and pectin as wound dressings, Int. J. Biol. Macromol. 124 (2019) 255–269.
[11] D. Chelminiak-Dudkiewicz, A. Smolarkiewicz-Wyczachowski, K. Mylkie, M. Wujak, D.T. Mlynarczyk, P. Nowak, S. Bocian, T. Goslinski, M. Ziegler-Borowska, Chitosan-based films with cannabis oil as a base material for wound dressing application, Sci. Rep. 12 (1) (2022) 18658.
[12] Y. Dong, M. Cui, J. Qu, X. Wang, S.H. Kwon, J. Barrera, N. Elvassore, G. C. Gurtner, Conformable hyaluronic acid hydrogel delivers adipose-derived stem cells and promotes regeneration of burn injury, Acta Biomater. 108 (2020) 56–66.
[13] P. Wang, S. Huang, Z. Hu, W. Yang, Y. Lan, J. Zhu, A. Hancharou, R. Guo, B. Tang, In situ formed anti-inflammatory hydrogel loading plasmid DNA encoding VEGF for burn wound healing, Acta Biomater. 100 (2019) 191–201.
[14] A. Sun, X. He, L. Li, T. Li, Q. Liu, X. Zhou, X. Ji, W. Li, Z. Qian, An injectable photopolymerized hydrogel with antimicrobial and biocompatible properties for infected skin regeneration, NPG Asia Mater. 12 (1) (2020) 25.
[15] H. Ying, J. Zhou, M. Wang, D. Su, Q. Ma, G. Lv, J. Chen, In situ formed collagen-hyaluronic acid hydrogel as biomimetic dressing for promoting spontaneous wound healing, Mater. Sci. Eng. C 101 (2019) 487–498.
[16] M.R. El-Aassar, O.M. Ibrahim, M.M.G. Fouda, N.G. El-Beheri, M.M. Agwa, Wound healing of nanofiber comprising polygalacturonic/hyaluronic acid embedded silver nanoparticles: in-vitro and in-vivo studies, Carbohydr. Polym. 238 (2020) 116175.
[17] G. Mutlu, S. Calamak, K. Ulubayram, E. Guven, Curcumin-loaded electrospun PHBV nanofibers as potential wound-dressing material, J. Drug Deliv. Sci. Technol. 43 (2018) 185–193.
[18] S. Homaeigohar, A.R. Boccaccini, Antibacterial biohybrid nanofibers for wound dressings, Acta Biomater. 107 (2020) 25–49.
[19] Y. Xie, Z.-x. Yi, J.-x. Wang, T.-g. Hou, Q. Jiang, Carboxymethyl konjac glucomannan - crosslinked chitosan sponges for wound dressing, Int. J. Biol. Macromol. 112 (2018) 1225–1233.
[20] A. Mohandas, B.S. Anisha, K.P. Chennazhi, R. Jayakumar, Chitosan-hyaluronic acid/VEGF loaded fibrin nanoparticles composite sponges for enhancing angiogenesis in wounds, Colloids Surf. B Biointerfaces 127 (2015) 105–113.
[21] X. Yang, C. Wang, Y. Liu, H. Niu, W. Zhao, J. Wang, K. Dai, Inherent antibacterial and instant swelling ε-poly-lysine/poly(ethylene glycol) diglycidyl ether superabsorbent for rapid hemostasis and bacterially infected wound healing, ACS Appl. Mater. Interfaces 13 (31) (2021) 36709–36721.
[22] Q. Jiang, B. Luo, Z. Wu, B. Gu, C. Xu, X. Li, X. Wang, Corn stalk/AgNPs modified chitin composite hemostatic sponge with high absorbency, rapid shape recovery and promoting wound healing ability, Chem. Eng. J. 421 (2021) 129815.
[23] C. Klinger, S. Żółtowska-Aksamitowska, M. Wysokowski, M.V. Tsurkan, R. Galli, I. Petrenko, T. Machałowski, A. Ereskovsky, R. Martinović, L. Muzychka, O. B. Smolii, N. Bechmann, V. Ivanenko, P.J. Schupp, T. Jesionowski, M. Giovine, Y. Joseph, S.R. Bornstein, A. Voronkina, H. Ehrlich, Express method for isolation of ready-to-use 3D chitin scaffolds from Aplysina archeri (Aplysineidae: Verongiida) demosponge, Mar. Drugs 17 (2) (2019) 131.
[24] S. Huang, X. Fu, Naturally derived materials-based cell and drug delivery systems in skin regeneration, J. Control. Release 142 (2) (2010) 149–159.

[25] A. Gaspar-Pintiliescu, A.-M. Stanciuc, O. Craciunescu, Natural composite dressings based on collagen, gelatin and plant bioactive compounds for wound healing: a review, Int. J. Biol. Macromol. 138 (2019) 854–865.
[26] M. Mir, M.N. Ali, A. Barakullah, A. Gulzar, M. Arshad, S. Fatima, M. Asad, Synthetic polymeric biomaterials for wound healing: a review, Progress Biomater. 7 (1) (2018) 1–21.
[27] P.B. Malafaya, G.A. Silva, R.L. Reis, Natural-origin polymers as carriers and scaffolds for biomolecules and cell delivery in tissue engineering applications, Adv. Drug Deliv. Rev. 59 (4–5) (2007) 207–233.
[28] T. Zhu, J. Mao, Y. Cheng, H. Liu, L. Lv, M. Ge, S. Li, J. Huang, Z. Chen, H. Li, L. Yang, Y. Lai, Recent progress of polysaccharide-based hydrogel interfaces for wound healing and tissue engineering, Adv. Mater. Interfaces 6 (17) (2019) 1900761.
[29] J. Combie, Properties of Levan and Potential Medical Uses, Polysaccharides for Drug Delivery and Pharmaceutical Applications, American Chemical Society, 2006, pp. 263–269.
[30] T. Zhan, Q. Bai, Z. Zhao, Antiproliferative effects of levan polysaccharide against colorectal cancer cells mediated through oxidative stress-stimulated HOTAIR/Akt signaling pathway: in vitro, Arab. J. Chem. 14 (12) (2021) 103389.
[31] G. Mummaleti, C. Sarma, S. Kalakandan, V. Sivanandham, A. Rawson, A. Anandharaj, Optimization and extraction of edible microbial polysaccharide from fresh coconut inflorescence sap: an alternative substrate, LWT 138 (2021) 110619.
[32] G.K. Ağçeli, N. Cihangir, Synthesis, characterization and antimicrobial performance of novel nanostructured biopolymer film based on Levan/clay/LL-37 antimicrobial peptide, Biocatal. Agric. Biotechnol. 23 (2020) 101421.
[33] D. Chelminiak-Dudkiewicz, A. Smolarkiewicz-Wyczachowski, K. Wegrzynowska-Drzymalska, M. Ziegler-Borowska, Effect of irradiation on structural changes of Levan, Int. J. Mol. Sci. 23 (5) (2022) 2463.
[34] D.S. Reddy, Therapeutic and clinical foundations of cannabidiol therapy for difficult-to-treat seizures in children and adults with refractory epilepsies, Exp. Neurol. 359 (2023) 114237.
[35] V. Golub, D.S. Reddy, Cannabidiol therapy for refractory epilepsy and seizure disorders, Adv. Exp. Med. Biol. 1264 (2021) 93–110.
[36] C. Bouter, F.W. Ott, D. Günther, L. Weig, F. Schmitz-Peiffer, M. Rozyyeva, N. Beindorff, Y. Bouter, Chronic exposure to a synthetic cannabinoid alters cerebral brain metabolism and causes long-lasting behavioral deficits in adult mice, J. Neural Transm. 130 (8) (2023) 1013–1027.
[37] E.P. Baron, Medicinal properties of cannabinoids, terpenes, and flavonoids in cannabis, and benefits in migraine, headache, and pain: an update on current evidence and cannabis science, Headache: The Journal of Head and Face Pain 58 (7) (2018) 1139–1186.
[38] H.C. Lu, K. Mackie, An introduction to the endogenous cannabinoid system, Biol. Psychiatry 79 (7) (2016) 516–525.
[39] S. Patel, M.N. Hill, J.F. Cheer, C.T. Wotjak, A. Holmes, The endocannabinoid system as a target for novel anxiolytic drugs, Neurosci. Biobehav. Rev. 76 (2017) 56–66.
[40] P. Kumar, D.K. Mahato, M. Kamle, R. Borah, B. Sharma, S. Pandhi, V. Tripathi, H. S. Yadav, S. Devi, U. Patil, J. Xiao, A.K. Mishra, Pharmacological properties, therapeutic potential, and legal status of *Cannabis sativa* L.: an overview, Phytother. Res. 35 (11) (2021) 6010–6029.
[41] B.D. Oomah, M. Busson, D.V. Godfrey, J.C.G. Drover, Characteristics of hemp (*Cannabis sativa* L.) seed oil, Food Chem. 76 (1) (2002) 33–43.
[42] X.Y. Lim, T.Y.C. Tan, S.H. Muhd Rosli, M.N.F. Sa'at, S. Sirdar Ali, A.F. Syed Mohamed, *Cannabis sativa* subsp. sativa's pharmacological properties and health effects: a scoping review of current evidence, PLOS ONE 16 (1) (2021), e0245471.
[43] Z. Zheng, J. Qi, L. Hu, D. Ouyang, H. Wang, Q. Sun, L. Lin, L. You, B. Tang, A cannabidiol-containing alginate based hydrogel as novel multifunctional wound dressing for promoting wound healing, Biomater. Adv. 134 (2022) 112560.
[44] P.K. Monou, A.M. Mamaligka, E.K. Tzimtzimis, D. Tzetzis, S. Vergkizi-Nikolakaki, I.S. Vizirianakis, E.G. Andriotis, G.K. Eleftheriadis, D.G. Fatouros, Fabrication and preliminary in vitro evaluation of 3D-printed alginate films with Cannabidiol (CBD) and Cannabigerol (CBG) nanoparticles for potential wound-healing applications, Pharmaceutics 14 (8) (2022) 1637.
[45] P.E. Antezana, S. Municoy, C.J. Pérez, M.F. Desimone, Collagen hydrogels loaded with silver nanoparticles and cannabis sativa oil, Antibiotics 10 (11) (2021) 1420.
[46] P.E. Antezana, S. Municoy, G. Orive, M.F. Desimone, Design of a new 3D gelatin—alginate scaffold loaded with cannabis sativa oil, Polymers 14 (21) (2022) 4506.
[47] D. Chelminiak-Dudkiewicz, P. Rybczynski, A. Smolarkiewicz-Wyczachowski, D. T. Mlynarczyk, K. Wegrzynowska-Drzymalska, A. Ilnicka, T. Goslinski, M. P. Marszałł, M. Ziegler-Borowska, Photosensitizing potential of tailored magnetite hybrid nanoparticles functionalized with Levan and zinc (II) phthalocyanine, Appl. Surf. Sci. 524 (2020) 146602.
[48] Z. Guo, Z. Zhang, N. Zhang, W. Gao, J. Li, Y. Pu, B. He, J. Xie, A Mg2+/ polydopamine composite hydrogel for the acceleration of infected wound healing, Bioact. Mater. 15 (2022) 203–213.
[49] Y. Liang, X. Zhao, P.X. Ma, B. Guo, Y. Du, X. Han, pH-responsive injectable hydrogels with mucosal adhesiveness based on chitosan-grafted-dihydrocaffeic acid and oxidized pullulan for localized drug delivery, J. Colloid Interface Sci. 536 (2019) 224–234.
[50] B. Dai, T. Cui, Y. Xu, S. Wu, Y. Li, W. Wang, S. Liu, J. Tang, L. Tang, Smart antifreeze hydrogels with abundant hydrogen bonding for conductive flexible sensors, Gels 8 (6) (2022) 374.
[51] H. Li, J. Yang, X. Hu, J. Liang, Y. Fan, X. Zhang, Superabsorbent polysaccharide hydrogels based on pullulan derivate as antibacterial release wound dressing, J. Biomed. Mater. Res. A 98 (1) (2011) 31–39.
[52] Y. He, W. Zhao, Z. Dong, Y. Ji, M. Li, Y. Hao, D. Zhang, C. Yuan, J. Deng, P. Zhao, Q. Zhou, A biodegradable antibacterial alginate/carboxymethyl chitosan/ Kangfuxin sponges for promoting blood coagulation and full-thickness wound healing, Int. J. Biol. Macromol. 167 (2021) 182–192.
[53] E. Kenawy, A.M. Omer, T.M. Tamer, M.A. Elmeligy, M.S.M. Eldin, Fabrication of biodegradable gelatin/chitosan/cinnamaldehyde crosslinked membranes for antibacterial wound dressing applications, Int. J. Biol. Macromol. 139 (2019) 440–448.
[54] B. Buyana, B.A. Aderibigbe, S.S. Ray, D.T. Ndinteh, Y.T. Fonkui, Development, characterization, and in vitro evaluation of water soluble poloxamer/pluronic-mastic gum-gum acacia-based wound dressing, J. Appl. Polym. Sci. 137 (21) (2020) 48728.
[55] B. Bozin, N. Mimica-Dukic, N. Simin, G. Anackov, Characterization of the volatile composition of essential oils of some lamiaceae spices and the antimicrobial and antioxidant activities of the entire oils, J. Agric. Food Chem. 54 (5) (2006) 1822–1828.
[56] N. Sakthiguru, M.A. Sithique, Fabrication of bioinspired chitosan/gelatin/ allantoin biocomposite film for wound dressing application, Int. J. Biol. Macromol. 152 (2020) 873–883.
[57] G. Mummaleti, C. Sarma, S.K. Kalakandan, H. Gazula, V. Sivanandham, A. Anandharaj, Characterization of Levan produced from coconut inflorescence sap using Bacillus subtilis and its application as a sweetener, LWT 154 (2022) 112697.
[58] I. Pantelić, M. Lukić, G. Gojgić-Cvijović, D. Jakovljević, I. Nikolić, D.J. Lunter, R. Daniels, S. Savić, Bacillus licheniformis Levan as a functional biopolymer in topical drug dosage forms: from basic colloidal considerations to actual pharmaceutical application, Eur. J. Pharm. Sci. 142 (2020) 105109.
[59] T. Demirci, M.E. Hasköylü, M.S. Eroğlu, J. Hemberger, E. Toksoy Öner, Levan-based hydrogels for controlled release of amphotericin B for dermal local antifungal therapy of candidiasis, Eur. J. Pharm. Sci. 145 (2020) 105255.
[60] S.S. Selvi, M.E. Hasköylü, S. Genç, E. Toksoy Öner, Synthesis and characterization of Levan hydrogels and their use for resveratrol release, J. Bioact. Compat. Polym. 36 (6) (2021) 464–480.
[61] H. Li, Q.-S. Zhao, S.-L. Chang, T.-R. Chang, M.-H. Tan, B. Zhao, Development of cannabidiol full-spectrum oil/2,6-di-O-methyl-β-cyclodextrin inclusion complex with enhanced water solubility, bioactivity, and thermal stability, J. Mol. Liq. 347 (2022) 118318.
[62] T. Zhou, S. Chen, X. Ding, Z. Hu, L. Cen, X. Zhang, Fabrication and characterization of collagen/PVA dual-layer membranes for periodontal bone regeneration, Front. Bioeng. Biotechnol. 9 (2021) 630977.
[63] Q. Li, F. Lu, G. Zhou, K. Yu, B. Lu, Y. Xiao, F. Dai, D. Wu, G. Lan, Silver inlaid with gold nanoparticle/chitosan wound dressing enhances antibacterial activity and porosity, and promotes wound healing, Biomacromolecules 18 (11) (2017) 3766–3775.
[64] G. Koşarsoy Ağçeli, N. Cihangir, Nano-sized biopolymer Levan: its antimicrobial, anti-biofilm and anti-cancer effects, Carbohydr. Res. 494 (2020) 108068.
[65] C.M.N. Mendonça, R.C. Oliveira, R.K.B. Freire, A.C.M. Piazentin, W.A. Pereira, E. J. Gudiña, D.V. Evtuguin, A. Converti, J.H.P.M. Santos, C. Nunes, L.R. Rodrigues, R.P.S. Oliveira, Characterization of Levan produced by a Paenibacillus sp. isolated from Brazilian crude oil, Int. J. Biol. Macromol. 186 (2021) 788–799.
[66] W. Xu, J. Peng, D. Ni, W. Zhang, H. Wu, W. Mu, Preparation, characterization and application of Levan/montmorillonite biocomposite and Levan/BSA nanoparticle, Carbohydr. Polym. 234 (2020) 115921.
[67] P.R.L. Dabare, A. Bachhuka, E. Parkinson-Lawrence, K. Vasilev, Surface nanotopography mediated albumin adsorption, unfolding and modulation of early innate immune responses, Mater. Today Adv. 12 (2021) 100187.
[68] K. Bialik-Wąs, K. Pluta, D. Malina, M. Barczewski, K. Malarz, A. Mrozek-Wilczkiewicz, Advanced SA/PVA-based hydrogel matrices with prolonged release of Aloe vera as promising wound dressings, Mater. Sci. Eng. C 120 (2021) 111667.
[69] R. Pereira, A. Carvalho, D.C. Vaz, M.H. Gil, A. Mendes, P. Bártolo, Development of novel alginate based hydrogel films for wound healing applications, Int. J. Biol. Macromol. 52 (2013) 221–230.
[70] K. Zhou, Z. Zhang, J. Xue, J. Shang, D. Ding, W. Zhang, Z. Liu, F. Yan, N. Cheng, Hybrid Ag nanoparticles/polyoxometalate-polydopamine nano-flowers loaded chitosan/gelatin hydrogel scaffolds with synergistic photothermal/ chemodynamic/Ag+ anti-bacterial action for accelerated wound healing, Int. J. Biol. Macromol. 221 (2022) 135–148.
[71] Q. Fang, Z. Yao, L. Feng, T. Liu, S. Wei, P. Xu, R. Guo, B. Cheng, X. Wang, Antibiotic-loaded chitosan-gelatin scaffolds for infected seawater immersion wound healing, Int. J. Biol. Macromol. 159 (2020) 1140–1155.
[72] K. Wegrzynowska-Drzymalska, D.T. Mlynarczyk, D. Chelminiak-Dudkiewicz, H. Kaczmarek, T. Goslinski, M. Ziegler-Borowska, Chitosan-gelatin films cross-linked with dialdehyde cellulose nanocrystals as potential materials for wound dressings, Int. J. Mol. Sci. 23 (17) (2022) 9700.
[73] J. Tavakoli, Y. Tang, Honey/PVA hybrid wound dressings with controlled release of antibiotics: structural, physico-mechanical and in-vitro biomedical studies, Mater. Sci. Eng. C 77 (2017) 318–325.
[74] W.G. Bae, D. Kim, M.K. Kwak, L. Ha, S.M. Kang, K.Y. Suh, Enhanced skin adhesive patch with modulus-tunable composite micropillars, Adv. Healthc. Mater. 2 (1) (2013) 109–113.
[75] T.M. Tamer, M.H. Alsehli, A.M. Omer, T.H. Afifi, M.M. Sabet, M.S. Mohy-Eldin, M.A. Hassan, Development of polyvinyl alcohol/kaolin sponges stimulated by

marjoram as hemostatic, antibacterial, and antioxidant dressings for wound healing promotion, Int. J. Mol. Sci. 22 (23) (2021) 13050.
[76] K. Ngece, B.A. Aderibigbe, D.T. Ndinteh, Y.T. Fonkui, P. Kumar, Alginate-gum acacia based sponges as potential wound dressings for exuding and bleeding wounds, Int. J. Biol. Macromol. 172 (2021) 350–359.
[77] S. Kaul, P. Sagar, R. Gupta, P. Garg, N. Priyadarshi, N.K. Singhal, Mechanobactericidal, gold nanostar hydrogel-based bandage for bacteria-infected skin wound healing, ACS Appl. Mater. Interfaces 14 (39) (2022) 44084–44097.
[78] T. Khaliq, M. Sohail, M.U. Minhas, S. Ahmed Shah, N. Jabeen, S. Khan, Z. Hussain, A. Mahmood, M. Kousar, H. Rashid, Self-crosslinked chitosan/κ-carrageenan-based biomimetic membranes to combat diabetic burn wound infections, Int. J. Biol. Macromol. 197 (2022) 157–168.
[79] M.F. do Nascimento, J.C. Cardoso, T.S. Santos, L.A. Tavares, T.N. Pashirova, P. Severino, E.B. Souto, R.L.C.d. Albuquerque-Junior, Development and characterization of biointeractive gelatin wound dressing based on extract of *Punica granatum* Linn, Pharmaceutics 12 (12) (2020) 1204.
[80] C. Su, H. Zhao, H. Yang, R. Chen, Stearic acid-modified starch/chitosan composite sponge with asymmetric and gradient wettability for wound dressing, ACS Appl. Bio Mater. 2 (1) (2019) 171–181.
[81] P. Deng, W. Jin, Z. Liu, M. Gao, J. Zhou, Novel multifunctional adenine-modified chitosan dressings for promoting wound healing, Carbohydr. Polym. 260 (2021) 117767.
[82] Z. Wu, W. Zhou, W. Deng, C. Xu, Y. Cai, X. Wang, Antibacterial and hemostatic thiol-modified chitosan-immobilized AgNPs composite sponges, ACS Appl. Mater. Interfaces 12 (18) (2020) 20307–20320.
[83] D. Morgan, What should a dressings formulary include?, in: Hospital Pharmacist-London 9(9), 2002, pp. 261–266.
[84] S. Güneş, F. Tıhmınlıoğlu, Hypericum perforatum incorporated chitosan films as potential bioactive wound dressing material, Int. J. Biol. Macromol. 102 (2017) 933–943.
[85] S. Koosehgol, M. Ebrahimian-Hosseinabadi, M. Alizadeh, A. Zamanian, Preparation and characterization of in situ chitosan/polyethylene glycol fumarate/thymol hydrogel as an effective wound dressing, Mater. Sci. Eng. C Mater. Biol. Appl. 79 (2017) 66–75.
[86] M. Li, Y. Liang, J. He, H. Zhang, B. Guo, Two-pronged strategy of biomechanically active and biochemically multifunctional hydrogel wound dressing to accelerate wound closure and wound healing, Chem. Mater. 32 (23) (2020) 9937–9953.
[87] A. Bouallegue, A. Casillo, F. Chaari, A. La Gatta, R. Lanzetta, M.M. Corsaro, R. Bachoual, S. Ellouz-Chaabouni, Levan from a new isolated Bacillus subtilis AF17: purification, structural analysis and antioxidant activities, Int. J. Biol. Macromol. 144 (2020) 316–324.
[88] O. Taylan, M.T. Yilmaz, E. Dertli, Partial characterization of a Levan type exopolysaccharide (EPS) produced by Leuconostoc mesenteroides showing immunostimulatory and antioxidant activities, Int. J. Biol. Macromol. 136 (2019) 436–444.
[89] J. Gallo, M. Raska, E. Kriegova, S.B. Goodman, Inflammation and its resolution and the musculoskeletal system, J. Orthop. Transl. 10 (2017) 52–67.
[90] R. Srikanth, G. Siddartha, C.H.S.S. Sundhar Reddy, B.S. Harish, M. Janaki Ramaiah, K.B. Uppuluri, Antioxidant and anti-inflammatory Levan produced from Acetobacter xylinum NCIM2526 and its statistical optimization, Carbohydr. Polym. 123 (2015) 8–16.
[91] M. Abbas, M. Arshad, M.K. Rafique, A.A. Altalhi, D.I. Saleh, M.A. Ayub, S. Sharif, M. Riaz, S.Z. Alshawwa, N. Masood, A. Nazir, M. Iqbal, Chitosan-polyvinyl alcohol membranes with improved antibacterial properties contained Calotropis procera extract as a robust wound healing agent, Arab. J. Chem. 15 (5) (2022) 103766.
[92] S. Dhanavel, E.A.K. Nivethaa, V. Narayanan, A. Stephen, In vitro cytotoxicity study of dual drug loaded chitosan/palladium nanocomposite towards HT-29 cancer cells, Mater. Sci. Eng. C Mater. Biol. Appl. 75 (2017) 1399–1410.
[93] K. Wang, J. Wang, L. Li, L. Xu, N. Feng, Y. Wang, X. Fei, J. Tian, Y. Li, Novel nonreleasing antibacterial hydrogel dressing by a one-pot method, ACS Biomater Sci. Eng. 6 (2) (2020) 1259–1268.
[94] H. Fang, J. Wang, L. Li, L. Xu, Y. Wu, Y. Wang, X. Fei, J. Tian, Y. Li, A novel high-strength poly(ionic liquid)/PVA hydrogel dressing for antibacterial applications, Chem. Eng. J. 365 (2019) 153–164.
[95] V. Serpooshan, M. Mahmoudi, M. Zhao, K. Wei, S. Sivanesan, K. Motamedchaboki, A.V. Malkovskiy, A.B. Gladstone, J.E. Cohen, P.C. Yang, J. Rajadas, D. Bernstein, Y.J. Woo, P. Ruiz-Lozano, Protein Corona influences cell-biomaterial interactions in nanostructured tissue engineering scaffolds, Adv. Funct. Mater. 25 (28) (2015) 4379–4389.
[96] B. Yang, Y. Chen, Z. Li, P. Tang, Y. Tang, Y. Zhang, X. Nie, C. Fang, X. Li, H. Zhang, Konjac glucomannan/polyvinyl alcohol nanofibers with enhanced skin healing properties by improving fibrinogen adsorption, Mater. Sci. Eng. C 110 (2020) 110718.
[97] E.V. Solovieva, A.Y. Fedotov, V.E. Mamonov, V.S. Komlev, A.A. Panteleyev, Fibrinogen-modified sodium alginate as a scaffold material for skin tissue engineering, Biomed. Mater. (Bristol, England) 13 (2) (2018) 025007.
[98] L.Y.C. Madruga, K.C. Popat, R.C. Balaban, M.J. Kipper, Enhanced blood coagulation and antibacterial activities of carboxymethyl-kappa-carrageenan-containing nanofibers, Carbohydr. Polym. 273 (2021) 118541.
[99] L. Zhang, B. Casey, D.K. Galanakis, C. Marmorat, S. Skoog, K. Vorvolakos, M. Simon, M.H. Rafailovich, The influence of surface chemistry on adsorbed fibrinogen conformation, orientation, fiber formation and platelet adhesion, Acta Biomater. 54 (2017) 164–174.
[100] A.A. Shitole, P. Raut, P. Giram, P. Rade, A. Khandwekar, B. Garnaik, N. Sharma, Poly (vinylpyrrolidone)-iodine engineered poly (ε-caprolactone) nanofibers as potential wound dressing materials, Mater. Sci. Eng. C 110 (2020) 110731.
[101] K. Kirketerp-Møller, P.Ø. Jensen, M. Fazli, K.G. Madsen, J. Pedersen, C. Moser, T. Tolker-Nielsen, N. Høiby, M. Givskov, T. Bjarnsholt, Distribution, organization, and ecology of bacteria in chronic wounds, J. Clin. Microbiol. 46 (8) (2008) 2717–2722.
[102] WHO, Global guidelines for the prevention of surgical site infection, second edition. https://www.who.int/publications/i/item/global-guidelines-for-the-prevention-of-surgical-site-infection-2nd-ed, 2018 (Accessed 06.02.2023).
[103] P.G. Bowler, B.I. Duerden, D.G. Armstrong, Wound microbiology and associated approaches to wound management, Clin. Microbiol. Rev. 14 (2) (2001) 244–269.
[104] Z. Pang, R. Raudonis, B.R. Glick, T.-J. Lin, Z. Cheng, Antibiotic resistance in Pseudomonas aeruginosa: mechanisms and alternative therapeutic strategies, Biotechnol. Adv. 37 (1) (2019) 177–192.
[105] M.P. Weinstein, J.S. Lewis, The clinical and laboratory standards institute subcommittee on antimicrobial susceptibility testing: background, organization, functions, and processes, J. Clin. Microbiol. 58 (3) (2020) (e01864-19).
[106] S.P. Denyer, J.Y. Maillard, Cellular impermeability and uptake of biocides and antibiotics in Gram-negative bacteria, J. Appl. Microbiol. 92 Suppl (2002) 35s–45s.
[107] M. Domżał-Kędzia, A. Lewińska, A. Jaromin, M. Weselski, R. Pluskota, M. Łukaszewicz, Fermentation parameters and conditions affecting Levan production and its potential applications in cosmetics, Bioorg. Chem. 93 (2019) 102787.
[108] K.H. Kim, C.B. Chung, Y.H. Kim, K.S. Kim, C.S. Han, C.H. Kim, Cosmeceutical properties of Levan produced by Zymomonas mobilis, J. Cosmet. Sci. 56 (6) (2005) 395–406.
[109] G.A.G. Legemaate, F.M. Burkle, J.J.L.M. Bierens, The evaluation of research methods during disaster exercises: applicability for improving disaster health management, Prehosp. Disaster Med. 27 (1) (2012) 18–26.
[110] W.H. Organization, Stability testing of active pharmaceutical ingredients and finished pharmaceutical products, WHO Technical report series 953 (2009) 87–123.